EurJOC
European Journal of Organic Chemistry

Minireviews
doi.org/10.1002/ejoc.202100372

Chemistry Europe
European Chemical Societies Publishing

VIP *Very Important Paper*

Special Collection

Catalysis in Supramolecular Systems: the Case of Gel Phases

Carla Rizzo,[a] Salvatore Marullo,[a] Floriana Billeci,[a] and Francesca D'Anna*[a]

Dedicated to Prof. Franco Cozzi *in the occasion of his 70th birthday.*

Supramolecular gels are a fascinating class of materials, originated by the self-assembly of low molecular weight molecules. Underpinned by non-covalent interactions, they find application in a diverse range of fields. Among these, supramolecular gels can be considered as organized, non-conventional reaction media, able to influence reactivity in a radically different way, compared with what happens in solution. This short review will focus on this aspect, covering literature from 2010 onwards, addressing the application of supramolecular gels as reaction media. In particular, in the first section we explore organocatalytic reactions in gel phase, with wide synthetic relevance, such as aldol and Mannich reactions as well as Friedel Crafts or ester hydrolysis processes. Subsequently, focus is laid on metal-catalysed reactions, among which relevance is given to widely used reactions like cross-coupling and click reactions. Then, the final sections describe the use of supramolecular gels as reaction media for photo- and biocatalysed processes.

Introduction

Nature is the main source of inspiration for supramolecular chemists and nature frequently performs chemical reactions in confined spaces. In terms of reactivity, a confined space having precise size and shape, can allow to control conformation and orientation of reagents, improve selectivity, control molecular size, exert microsolvent effect and protect unstable intermediate or products. This is the reason why reactions in confined media are currently gaining much interest.[1]

Among systems that supramolecular chemistry suggests as confined reaction media, cavitand hosts play a significant role. Consequently, in the last decades, non-biological host molecules have included zeolites,[2] metal-organic frameworks,[3] metal-organic cages,[4] cyclodextrins,[5] cucurbiturils,[6] nanotubes,[7] fullerenes[8] and so on.

Beside above examples, also systems derived from supramolecular aggregation processes proved to be interesting as, in some cases, together with significant effects on the kinetic of the target reactions, they can also give rise to effects of chirality amplification.[9]

Among self-assembled supramolecular systems active in catalysis, supramolecular gels are valuable tools. They are obtained from aggregation processes occurring among low molecular weight compounds (LMWCs) that give rise to a fibrillary network (SAFIN), able to trap solvent molecules. The SAFIN is built as result of the establishment of feeble and cooperative supramolecular interactions that are reversible in nature. With respect to the above considered cavitand hosts, in the case of supramolecular gels, the confined space forms under suitable experimental conditions. Consequently, the action of suitable stimuli can act on the assembly-disassembly equilibrium allowing to conveniently modulate the state of the system.

One of the main classifications of supramolecular gels is based on the nature of the hardened solvent. Then, a clear distinction among hydro-, organo-, iono- and eutectogels is used when trapped solvents are water, organic solvents, ionic liquids or deep eutectic solvents, respectively.

The empty spaces featuring these soft materials endow them with a high porosity that warrants their wide range of applications. Consequently, supramolecular gels have been used in environmental remediation[10] and preservation processes,[11] as sensors,[12] as drug delivery systems,[13] but also as supramolecular reaction media. In the latter case, they show several advantages as the well-ordered arrangement of gelator molecules could impart enhanced efficiency to catalytic groups as a consequence of their proximity and conformational restrictions. The reversible nature of supramolecular interactions could give rise to tunable catalytic activity. Finally, in some cases, supramolecular catalytic gels could behave as supported catalysts and, thanks to their semi-solid nature could be filtered at the end of the process, carefully washed and reused. This latter aspect has significant positive repercussions from an environmental point of view.

The last decade has witnessed a raise in interest on the possibility of using supramolecular gels as organized reaction media and some interesting review papers have been already published in the years.[14]

This review devotes its attention to the literature covering the range 2010–2020. In particular, applications of

[a] *Dr. C. Rizzo, Dr. S. Marullo, Dr. F. Billeci, Prof. F. D'Anna*
Università degli Studi di Palermo, Dipartimento STEBICEF
Viale delle Scienze, Ed. 17, 90128 Palermo, Italy
E-mail: francesca.danna@unipa.it
https://www.unipa.it/persone/docenti/d/francesca.danna/en/?pagina=-curriculum

Special Collection *Part of the "Franco Cozzi's 70th Birthday" Special Collection.*

supramolecular gels in organocatalysis, metal catalysis, photocatalysis and biocatalysis are considered. Obviously, the analysis is not exhaustive but could represent a good support to researchers working in the field.

Organocatalysis

Among the reactions studied in gel phases, the aldol reaction is one of the most widely investigated. The interest in such kind of reaction comes from its resemblance to prebiotic chemistry, that starting from simple components, allows the obtainment of sugars and complex carbohydrates. In this context, small amino acids and peptides have been used as catalysts and tested both in solution and gel phase. Their use in gel phase, especially in the case of hydrogels, might be of relevance as the gel environment is similar to cytoplasm interior.

In most cases, the aldol reaction between *p*-nitrobenzaldehyde and cyclohexanone has been chosen as benchmark reaction. In one of the first examples, the amphiphilic peptide **ProValC$_{12}$** was used as gelator to obtain hydrogel at 2 mM (Scheme 1A).[15]

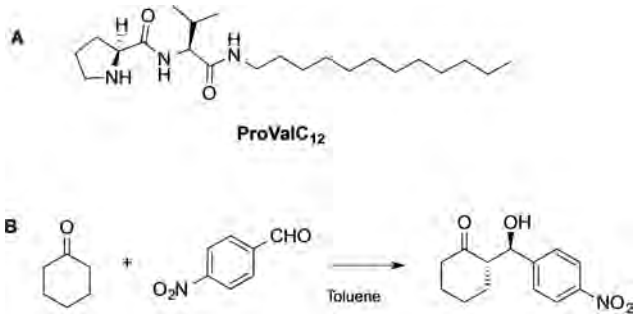

Scheme 1. A) Structure of **ProValC$_{12}$** gelator and **B)** schematic representation of the aldol reaction.

The reaction was performed using different approaches, like the placement of neat reagents on the top of the gel or their addition to the gel phase as concentrated toluene solution. In the first case, quantitative yield was obtained, after 36 h at 25 °C, with moderate diastereoselectivity (*anti*:*syn*, 75:25) and poor enantioselectivity (*ee*: 12%). Differently, the use of toluene solution decreased reaction time (16 h), improved diastereose-

Francesca D'Anna was born in Palermo in 1972. She received her chemistry degree in 1997 from the University of Palermo, discussing a graduation thesis in the field of physical organic chemistry. In February 2003 she obtained her PhD, discussing a thesis on "Host-Guest Systems Formed by Cyclodextrins. Recognition and Transformation of Organic Substrates", under the supervision of Prof. R. Noto. Since 2003 she has been working at the Chemistry Division of STEBICEF Department of the University of Palermo and from March 2021 she is Full Professor of Organic Chemistry. Her interests lie in the study of ionic liquids' properties and applications, supramolecular chemistry, and study of the gelling behavior of organic salts. She is author of more of than 110 publications and 9 reviews.

Salvatore Marullo was born in 1980 in Agrigento, Italy. In 2008 he received his Ph.D. in Chemistry at the University of Palermo under the supervision of Prof. V. Frenna and Prof. F. D'Anna. In 2013 he did a post-doctoral research stay at the University of York, UK, under the supervision of Prof. D. K. Smith and since 2014 he is a researcher in Organic Chemistry at the STEBICEF department of the University of Palermo, working in the group of Prof. F. D'Anna. His research interest is mainly focused on Ionic Liquids and Deep Eutectic Solvents Synthesis, properties and catalytic ability especially for biomass transformation in products of industrial value, as well as on Supramolecular Self-Assembly processes.

Carla Rizzo was born in Palermo in 1988. She received her MSc degree in Chemistry in 2012 and her PhD in 2016 at the University of Palermo, both under the supervision of Prof. F. D'Anna and Prof. R. Noto. During her formation, she spent two research periods abroad at QUILL, of the Queen's University of Belfast and at Georgetown University, Washington, DC, USA. She obtained several post-doctoral positions at the University of Palermo and, in 2017, she has been a visiting post-doctoral researcher at Durham University, working with Prof. J. W. Steed. Her research activity is mainly focused on Ionic Liquids synthesis, properties and catalytic ability as well as on Supramolecular Gels formation and their possible use for environmental remediation, catalysis or biological applications.

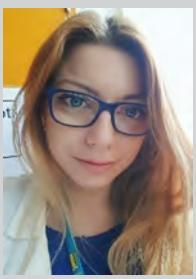

Floriana Billeci was born in Palermo in 1989, and she graduated at the University of Palermo with both BSc and MSc degrees in Chemistry. She studied for her PhD at the University of Palermo and in QUILL, at the Queen's University of Belfast, achieving PhD Degree in February 2019, under the supervision of Prof. F. D'Anna, Prof. K. R. Seddon, Dr. H. Q. N. Gunaratne and Dr. N. V. Plechkova. She has focused her research on Green Chemistry, in particular in the field of Ionic Liquids, studying their synthesis and application in the environmental prevention and protection fields, publishing some papers. In this regard, she also worked on a research project at the University of Nottingham under the supervision of Prof. P. Licence and, recently, she has been part of a research project on new catalytic systems with the CINMPIS consortium.

lectivity (*anti*:*syn*, 91:9), but left enantioselectivity unchanged (*ee*: 18%). From a stereochemical point of view, the performance of the reaction was improved by temperature decrease and, at 5 °C, a significant increase in *ee*, (*S*,*R*)-*anti* (88%) was obtained. To certainly identify the reaction site, gel and toluene phase were left to stand in contact for prolonged times. ^{1}H NMR analysis of organic phase demonstrated the absence of gelator molecules in the organic phase, allowing to ascribe the catalytic activity to the restricted mobility of the reactants and the structural rigidification of the catalytic supramolecular aggregates. Interestingly, the gel phase was reused three times without loss in efficiency.

To better understand the reasons inducing the lack of stereoselectivity, the aldol reaction between acetone and *p*-nitrobenzaldehyde was performed in gel phases formed by bolaamphiphilic gelators **(ProVal)C$_n$** in ACN, at −20 °C (Scheme 2).[16]

The comparison between data collected in gel phases and in ACN solution for **ProValC$_3$** (Scheme 2), which is not able to harden the organic solvent, demonstrates that the racemization process occurs only in gel phase and proceeded on the formed aldol as a consequence of the high acidity of benzylic protons. Evidence about the higher basicity of gel phases with respect to the corresponding solutions, were obtained comparing change in color for some selected indicators as a function of the temperature (Scheme 3). This was ascribed to the close proximity of the pyrrolidinic units of the L-proline on the gel surface.

The reaction between cyclohexanone and *p*-nitrobenzaldehyde has been also used as a probe to assess the relevance of the aggregation degree on the catalytic activity. To this aim, short lipophilic peptides featured by the presence of L-proline unit and bearing the alternating sequence phenylalanine (F)-glutammic acid (E) were used to facilitate their assembly into β-sheet structures (Scheme 4).[17]

Peptides also bore or lacked hydrophobic alkyl chain at the C-terminus (**PFEC$_3$**, **PFEC$_{12}$**, **PEFC$_3$** and **PEFC$_{12}$**; **P(FE)$_4$ANH$_2$**, **P(EF)$_4$ANH$_2$**, respectively). The above structural features gave rise to the obtainment of compounds highly soluble in water (**PFEC$_3$** and **PEFC$_3$**) or able to harden phosphate buffer at p*H* = 7 (**PFEC$_{12}$**, **PEFC$_{12}$**, **P(FE)$_4$ANH$_2$**, **P(EF)$_4$ANH$_2$**). Only gel phases were able to catalyze the target reaction, with differences in yield values that significantly depended on the structure of the used gelator. In particular, the differences were ascribed to the nature of neighboring L-proline, with L-phenylalanine giving better performance with respect to glutamic acid (yield: 93 and 51% in the presence of **PEFC$_{12}$** and **PEFC$_{12}$** at t = 2 h, respectively) and the presence or absence of the hydrophobic tail. In particular, more hydrophilic peptides, **P(FE)$_4$ANH$_2$** and **P(EF)$_4$ANH$_2$**, gave incomplete conversion also after 72 h. A detailed ^{1}H NMR investigation allowed identifying the incorporation of the cyclohexanone in the aggregated phase as the key factor determining the outcome of the reaction, that in turn depends on the hydrophobicity of the environment. A higher incorporation warranted a major enamine intermediate formation, that drives the reaction. This was supported by the shift detected for emission band of 1-anilino-naphthalene-8-sulphonate (ANS), a probe widely used to track hydrophobic regions in proteins.

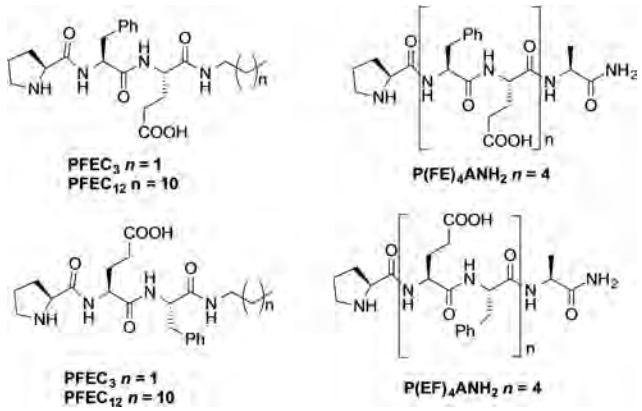

Scheme 4. Structures of lipophilic peptides.

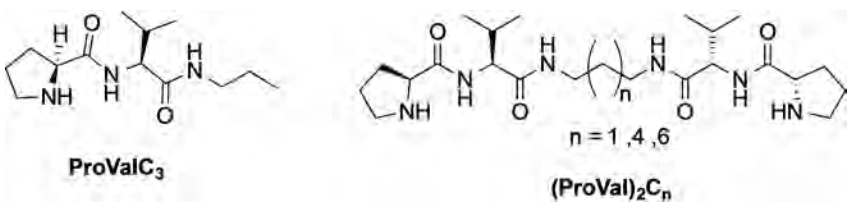

Scheme 2. Structure of bolaamphiphilic gelators.

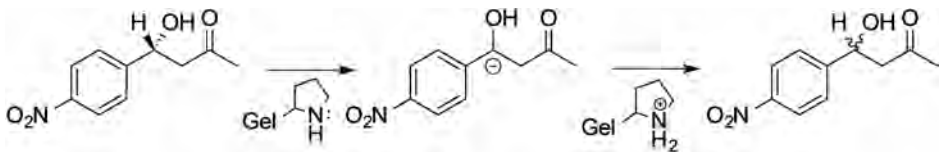

Scheme 3. Suggested mechanism for the racemization process in gel phase.

Interestingly, the best catalytic gel phases (**PEFC$_{12}$** and **PEFC$_{12}$**) were also tested in the condensation of several α-oxy-aldehyde and phenylalkylaldehydes to mimic prebiotic chemistry (Scheme 5).

Also in this case, better performance was obtained with less polar substrates, confirming the hypothesis that a hydrophobic environment of fibers is needed to store the substrate near to the catalytic site.

In a different study, a tandem deacetylation/aldol probe reaction, between dimethylacetaldehyde and cyclohexanone, was used to study the effect of self-sorting of fibers in gel phases formed by **(SucVal)$_2$C$_8$**, **ProValC$_{12}$**, and **(ProVal)$_2$C$_8$**[18] (Scheme 6).

This approach, known as orthogonal self-assembly process, was used with the aim to allow the spatial separation of two incompatible catalytic moieties inside the gel network (the proline unit of the **ProValC$_{12}$** and **(ProVal)$_2$C$_8$** and the carboxylic unit of **(SucVal)$_2$C$_8$**). The co-assembled systems showed different structural features. Indeed, a combined approach of morphological, rheological and thermal investigation demonstrated that while the addition of increasing amounts of **ProValC$_{12}$** to **(SucVal)$_2$C$_8$** induced the formation of mechanically stronger hydrogels, with increased thermal stability and mixed morphological motifs, the addition of **(ProVal)$_2$C$_8$** to **(SucVal)$_2$C$_8$** caused the formation of mechanically feebler hydrogels with a homogeneous fibrous structure. Interestingly, different structural features of mixed hydrogels gave rise to different catalytic activity. Indeed, **(SucVal)$_2$C$_8$/ProValC$_{12}$** hydrogels (7 mM) were able to catalyze the tandem reaction to give, after 72 h, 85% of yield in aldol product, with *anti:syn* ratio 84:16 and *ee* equal to 90%. Such results proved comparable to the ones obtained using benzaldehyde as starting material in the same gel system, indicating that deacetylation reaction was not the rate limiting step.

Differently, when **(SucVal)$_2$C$_8$/ProValC$_8$** bicomponent gel was used, after 96 h, only the conversion of 58% of benzaldehyde dimethylaceta was observed without aldol formation, showing in this case the occurrence of a salt bridge that prevents the formation of enamine intermediate needed for the catalysis of the aldol reaction.

More recently, Smith *et al.* using a glutanamide derivative (**GluC$_{12}$**) to catalyse the aldol reaction between *p*-nitrobenzaldehyde and cyclohexanone in aqueous solution, observed that reagents addition induced the formation of a gel-like phase (Scheme 7).[19]

Deep investigation of the observed phenomenon demonstrated that gel phase resulted from the formation of the reversible imine intermediate between **GluC$_{12}$** and *p*-nitrobenzaldehyde. This adduct behaved as a supergelator, being able to induce gel phase formation at concentration lower than 0.1% w/vol. The system exhibited self-sorting behavior as the two-component gel phase formed only in the presence of electron withdrawing substituted aromatic aldehydes. The two-component gel, formed in the reaction mixture, showed enhanced catalytic activity in the benchmark reaction, with conversion up to 98%, after 72 h, *anti:syn* ratio 2.1:1.0 and modest *ee* for the *anti* stereoisomer (32%).

In addition, also the secondary amine obtained from the *in situ* reduction of the imine intermediate with $NaBH_4$, exhibited gelling behavior, both in water and in buffer solution at p*H* = 7.4. Its use in the organocatalyzed dimerization of glycolaldehyde allowed obtaining conversion to threose and erythrose ranging from 43 up to 76%, with significant selectivity towards threose over erythrose (2:1) and a small *ee* in favor of L-threose (6.5%) and L-erythrose (2.5%). Among organocatalyzed reactions also the Henry reaction, between aromatic aldehydes and nitroalkanes, has been investigated in organogel phases. To this aim, the dimeric **(ProVal)$_2$C$_8$** gelator was tested for its gelling ability in nitroalkanes, such as nitromethane and nitroethane, and the corresponding organogels were employed to catalyze the reaction in the presence of *p*-substitutued benzaldehydes (Schemes 6 and 8).[20]

Data collected, at 20 °C, shed light on very interesting aspects. Firstly, the reaction proceeded only in gel phases and not in diluted solution of gelator. Substrate conversion was equal to 99 and 15% in gel and solution phase, respectively. This was ascribed to the enhanced basicity of the L-Pro moiety in the aggregated phase, as accounted for by the change in color of the bromothymol blue in gel phase with respect to the diluted solution of the catalyst. However, reaction in gel phase did not show stereochemical advantage, differently from the

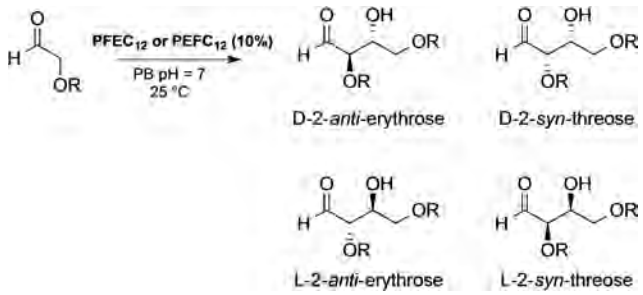

Scheme 5. Representation of self-condensation of α-oxy-aldehydes.

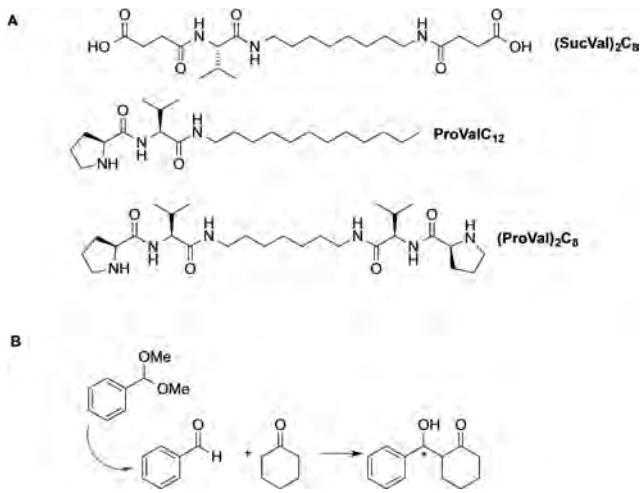

Scheme 6. A) Structure of gelators used in self-sorting process and **B)** representation of tandem deacetylation/aldol reaction.

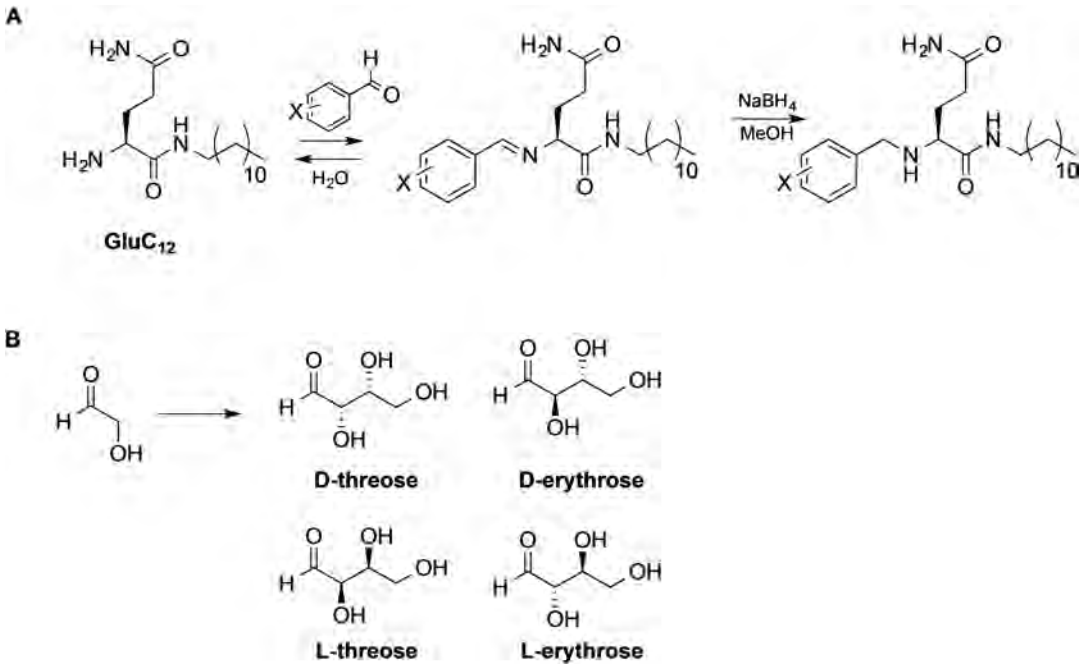

Scheme 7. A) Schematic representation of imine intermediate and its reduction; **B)** representation of the gel catalyzed dimerization of glycolaldehyde.

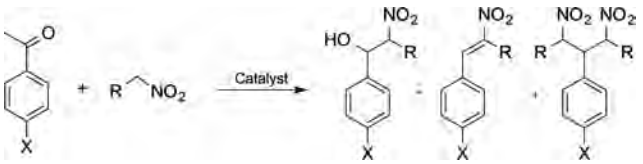

Scheme 8. Schematic representation of the Henry reaction.

aldol reaction performed in gel phases formed by the same family of gelators. On the other hand, when the reaction was conducted in solution, dehydration and conjugated addition of by-products were detected (Scheme 8).

The increase in the catalyst basicity also induced a shift of the mechanism. The reaction proceeded through ion pair mechanism in gel phase and by the iminium intermediate in solution. Interestingly, the mechanism switch proved affected by the electronic nature of the substituent on the aromatic moiety, with the ion pair one favored in the presence of electron withdrawing substituents.

Different results were also collected in dependence of the nature of the gelation solvent. In particular, gel formed in nitrometane gave lower conversion values and only a low yield in alkene, accounting for a "gel effect". This latter was considered the result of the different arrangement of the microcrystalline structure of the gel.

The role played by the bolaamphiphilic gelator **(ProVal)$_2$C$_6$** (Scheme 2) was deeply investigated using as probe reaction the 1,4-conjugated addition of cyclohexanone to *trans*-β-nitrostyrene (Scheme 9).[21]

Data collected in gel phase, formed in toluene, were compared to the ones obtained in aggregated solution of **ProValC$_3$** (Scheme 2) and non-aggregated solution of the prolinamide analogue **ProC$_3$**. Higher yields at room temperature were obtained in gel phase and aggregate solution. The highly organized structure allowed the obtainment of the highest diastereoselectivity (98:2; *syn*/*anti*) and enantioselectivity (34%; *2R*, *1'S*). Interestingly, investigation performed to evaluate the effect of the catalyst concentration and temperature on the *ee*, evidenced that in both cases the most significant effects were detected in the presence of **ProValC$_3$**. In particular, stereoselectivity inversion was detected. The above phenomenon was ascribed to the different states featuring **ProValC$_3$** solution as a function of the concentration (solution-aggregates) and tem-

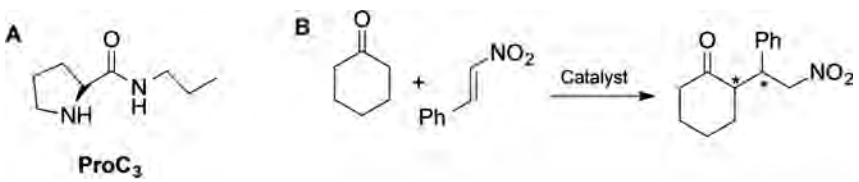

Scheme 9. A) Structure of prolinamide **ProC$_3$**; **B)** schematic representation of the 1,4-conjugate addition.

perature (aggregates-solution). A deep NMR and X-ray investigation shed light on the thick texture of hydrogen bond featuring aggregates and gel phase. The L-proline moiety, being involved in the intramolecular hydrogen bond with the N–H of the close amide moiety, was not able to give the enamine intermediate, but acted as a base, favoring the enolate formation.

The effect of self-sorting of fibers formed by **ProValC$_{12}$** (Scheme 1), **(ProVal)$_2$C$_8$** and **(SucVal)$_2$C$_8$** (Scheme 6) was also tested on the catalysis of the stereoselective Mannich reaction among benzaldehyde, aniline and cyclohexanone (Scheme 10).[22]

All peptides were able to form hydrogels and, in all case, the amount of gelator present, as free molecules in the gel network, was evaluated by ^{1}H NMR investigation. All gelators, in solution, catalyzed the *anti*-selective Mannich reaction with **ProValC$_{12}$** being the most efficient catalyst, as accounted for by the highest reaction rate ($4.0 \pm 0.1 \cdot 10^{-5}$) s^{-1}, yield (90%) and diastereoselectivity for the *anti*-product (*anti*/*syn* 90:10), with the obtainment of the major diastereoisomer in racemic mixture. The attempt to carry out the reaction by mixing different gelator molecules gave rise to different results as a consequence of the nature of the substrates and molar ratios used. In particular, self-sorting of **ProValC$_{12}$** and **(SucVal)$_2$C$_8$** in comparable amount did not induce improvements with respect to fibrous system of **ProValC$_{12}$**. Differently, when a gelatinous network of **ProValC$_{12}$** (6 mM) was built in the presence of **(SucVal)$_2$C$_8$** (1 mM), a significant improvement in both diastero- (*anti*/*syn* 95:5) and enantioselectivity (85:15) was detected. The above result was ascribed to the ability of free molecules of **(SucVal)$_2$C$_8$** to share the acidic proton with the amine intermediate in the transition state, resulting in a drastic improvement of the enantiomeric excess. Conversely, when structurally similar hydrogelators, **(SucVal)$_2$C$_8$** and **(ProVal)$_2$C$_8$**, were self-sorted, in comparable or different amounts, no significant improvement in the overall stereoselectivity was observed, as a consequence of the similar efficiency and poor stereoselectivity of both catalysts. This pointed out the need to have catalysts of very different activity as components of a self-sorted gelatinous network, to induce the less efficient catalyst to act as a promoter for the reaction outcome, giving rise to formation of the preferred product.

Metal-free Friedel Craft reaction has been performed in gel phases obtained from the self-assembly process of *N*,*N*′-disubstituted urea-based catalysts in conventional organic solvents (Scheme 11).[23]

Interestingly, properties of organogels were greatly affected by the nature of the substituents borne on the urea or thiourea structural motifs. Analysis of physico-chemical properties of gel phases, combined with quantum-mechanical investigation, allowed to identify π-π stacking and hydrogen bond as main driving forces of the gelation process. The gel formed by **G1** in toluene was used as reaction vessel for the alkylation of 1-*H*-indole with trans-β-nitrostyrene.

The comparison between data collected in solution and in gel phase evidenced the positive effect of the gelationous network on the outcome of the reaction, as accounted for by the increase in both yield and *ee* (yield: 36 and 60%; *ee*: 16 and 21 for solution and gel phase). This was ascribed to the possibility that fibrillar network could provide catalyst spatial isolation and shielding effect responsible for the increase in yield and facial discrimination.

Evidences about the favourable effect that the three-dimensional network of a gel phase can exert on the outcome of the aldol reaction have been also reported in the case of soft materials formed in ionic liquid solution.[24] Indeed, in the attempt to optimize conditions of the reaction between acetone and *p*-nitrobenzaldehyde, in the presence of L-proline, the formation of ionogel phase was observed when a weight ratio [bmim][Cl]/acetone 80:20 and a [bmim][Cl]/L-proline 32.6:1 was used (Scheme 12).

Interestingly, in gel phase the reaction proceeded with 90% of yield and 62% of *ee*. This result was ascribed to the supramolecular structure formed by the interactions established among L-proline and ions constituting the ionic liquid, that provide the appropriate mass transfer for the catalytic process.

Ionogels have been also used to perform the asymmetric alcoholysis of anhydrides in the presence of Cinchona alkaloid derivatives. To this aim, gel phases obtained from the gelation of dicationic organic salt, **[*p*-C$_{12}$Im]$_2$[Edta]**, in [bmim][BF_4], [bmim][NTf_2] and [bmpyrr][NTf_2] were used (Scheme 13).[10c]

In the absence of catalyst, at 4 °C for 24 h, the yield in product increased on going from ionic liquids to gel phases and the best yield was obtained in the ionogel featured by the presence of more flexible network, **[*p*-C$_{12}$Im]$_2$[Edta]**/[bmim][NTf_2], as accounted for by rheological parameters. With the best gel in hand, the effect of **MQ** organocatalyst was tested also changing the alcohol nature. In all cases, a positive effect of the catalyst was detected. Once again, the reaction in gel phase gave higher yields with with respect to the corresponding ionic liquid solution, but the increase in yield due to the presence of the organocatalyst resulted higher in solution than in gel phase. This result was ascribed to the modification of the gel structure by the alkaloid component that changes the diffusion rate of the alcohol in the gel structure.

As far as the *ee* is concerned, good values ranging from 61 up to 81% were obtained performing the reaction in gel phase at −30 °C and for 48 h. The enhanced enantioselectivity in the above conditions was ascribed to the action of the "asymmetric environment" in gel phase that decreased both diffusion and conformational exchange rates.

The use of ionogels as reaction media has been also tested to perform the Baylis-Hilmann reaction between 4-fluorobenzaldehyde and methylacrilate (Scheme 14).[25]

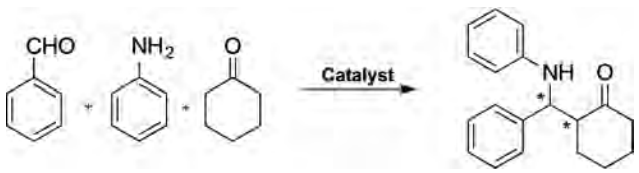

Scheme 10. Representation of the stereoselective Mannich reaction.

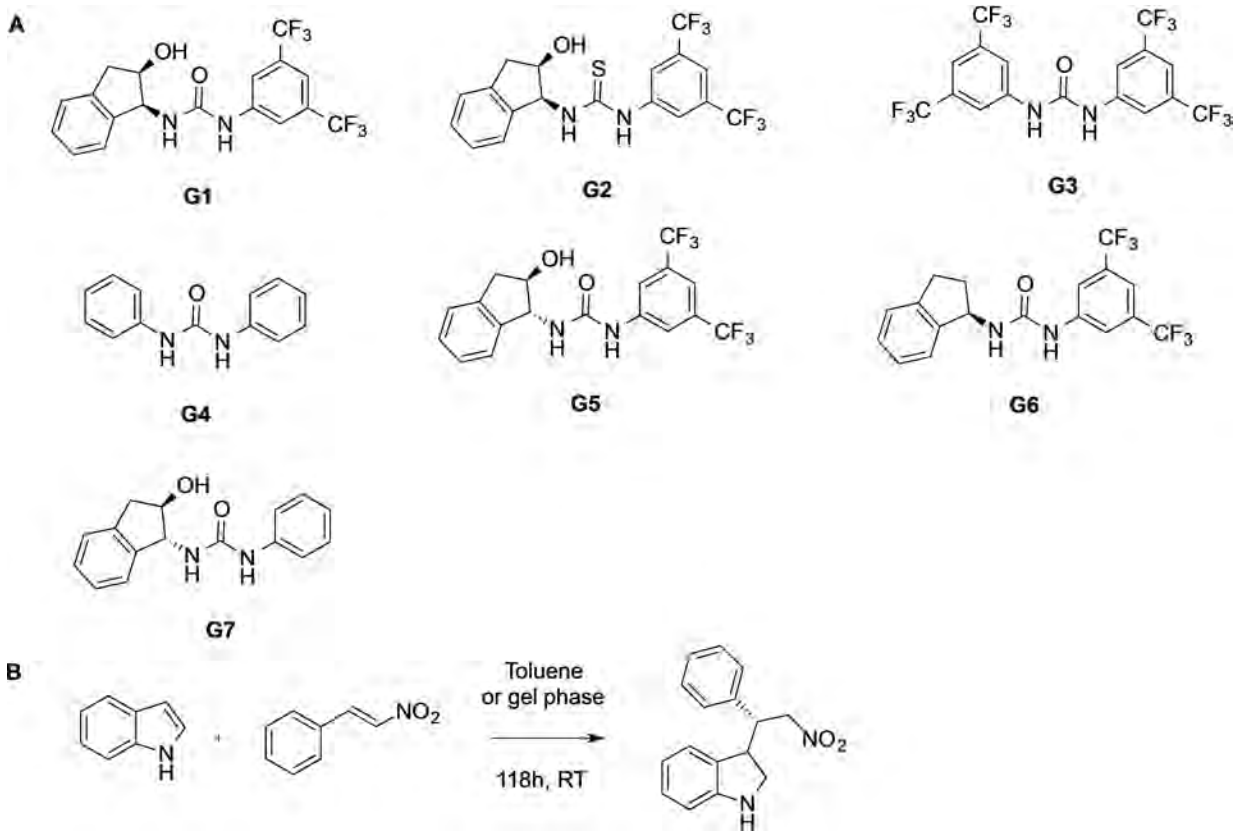

Scheme 11. A) Gelator structures; **B)** schematic representation of the alkylation of 1*H*-indole with trans-β-nitrostyrene.

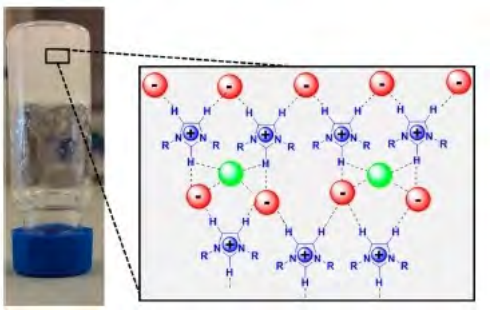

Scheme 12. Gel phase obtained in the presence of a [bmim][Cl]/L-proline at 32.6:1 weight ratio. Reproduced from Ref. [24], Copyright (2016), with permission from American Chemical Society.

The reaction was performed in the gel phase obtained from the **N-Boc-L-Phe-C_{16}** in [bmim][PF_6], at 3.5 wt%, in the presence of 1 eq. of DABCO as base catalyst. The reactive ionogel was prepared by incorporation of all reagents in the gel network and comparison between rheological data obtained for pristine and doped gel showed that the presence of the reagents induced a decrease in the stiffness of the gel. Conversion of 76% with yield of 75% were obtained at room temperature, using a reaction time of 24 h. Unfortunately, no enantioselectivity was detected and performance of the reaction did not improve by increasing the reaction time or amount of gelator. The reaction proceeded well in the presence of different aldehydes and reaction rates, in the non-stirred ionogel, resulted comparable to the one detected in solution, notwithstanding the significant increase in the viscosity of the reaction media. This was mainly ascribed to the increase in the local concentration of the reagents in the gelatinous network that favors the progress of the reaction.

In the attempt to mimic enzymatic catalysis and, in particular esterase activity, low molecular weight gelators bearing appended imidazole moieties, **(ImVal)$_2$C$_8$** and **Im$_2$C$_8$**, were prepared and tested for the hydrolysis of both activate (*p*-nitroacetate methylester) and non-activated esters (L- and D-phenylalanine methylesters) (Scheme 15).[26]

The presence of the Val residue on the gelator structure proved to be essential to drive the self-assembly process and hydrogel formation. pK_a measurements showed that, upon assembly and gelation, one of the imidazole moieties of the gelator molecule undergoes basicity enhancement. The resulting hydrogel promoted fast hydrolysis of *p*-nitrophenylacetate as well as of inactivated esters. Catalytic activity depended on the p*H* value, with the best performance obtained at p*H* = 6 and 6.5.

Under identical conditions, hydrolysis occurred much more slowly in the presence of the non-gelling analogue, **Im$_2$C$_8$**. Therefore, the rate-enhancing effect of the hydrogel was ascribed to the high concentration of catalytic sites within the

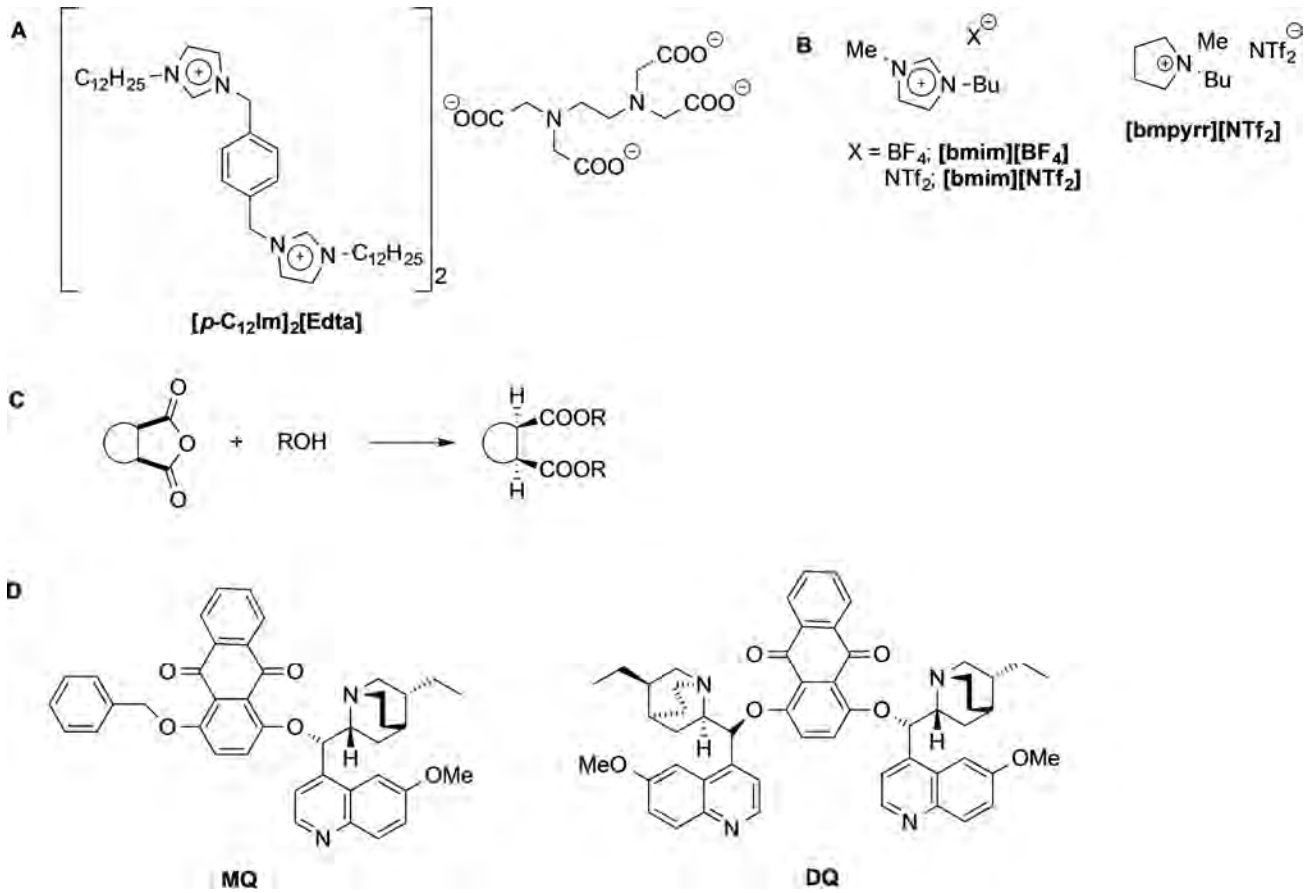

Scheme 13. A) Gelator structure; **B)** ionic liquid structures; **C)** schematic representation of the alcoholysis reaction; **D)** organocatalyst structures.

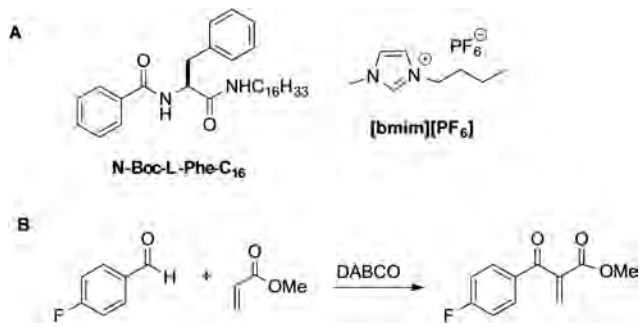

Scheme 14. Representation of **A)** gelator and ionic liquid structure, and **B)** Baylis-Hilmann reaction.

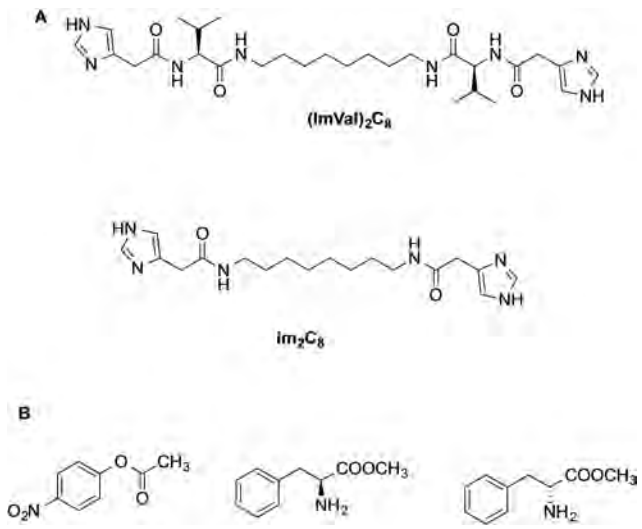

Scheme 15. A) Structure of hydrogelator, non-gelling analogue and **B)** ester substrates.

gel network, to the presence of hydrophobic pockets and the cooperativity between both unprotonated and protonated imidazole moieties. A combined approach of TEM, IR and CD investigation demonstrated that increasing the p*H* from 6 up to 7, induced a significant variation in the gel morphology, that changed from fibrous to flat belt-like structure. Analogously, the evaluation of the environment hydrophobicity, as accounted for by spectral shift of ANS allowed foreseeing the formation of hydrophobic pocket at p*H* = 6.0, that bound more efficiently the substrate and favored the outcome of the reaction.

In another example, the aggregation behavior of a synthetic flavin catalyst has been studied to have systems able to

simulate enzymatic function of flavin-containing oxygenase and oxidase. To this aim, sonication of octadecanoyl derivative, **C_{18}Rbf-CH_3**, in organic solvents, gave rise to the formation of opaque organogels (Scheme 16).[27]

Soft materials obtained exhibited structural features dependent on the sonication time, as accounted for by the gelation times as well as the size of the spherical aggregates featuring gel phases. The organogel obtained in butanenitrile, at 0.015 M, was used as reaction media to perform the aerobic reduction of olefins in the presence of $NH_2NH_2 \cdot H_2O$ at room temperature. With respect to the non-aggregated flavin derivative **C_{16}Rbf**, **C_{18}Rbf-CH_3** showed substrate specificity with reduction of aliphatic olefins occurring faster than the corresponding aromatic substrates. This was ascribed to the higher ability of the aliphatic substrate to interact with the artificial cavity formed by the aggregation of the riboflavin derivative. Then the so formed supramolecular complex undergoes reduction with NH_2NH_2. Interestingly, the reactivity trend detected in gel phase reverses the one previously observed in the presence of dendrimeric derivatives of **C_{18}Rbf-CH_3**.

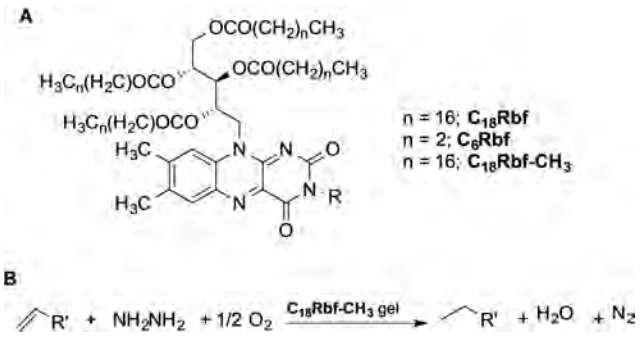

Scheme 16. A) Structures of riboflavin catalysts; **B)** schematic representation of olefins reduction.

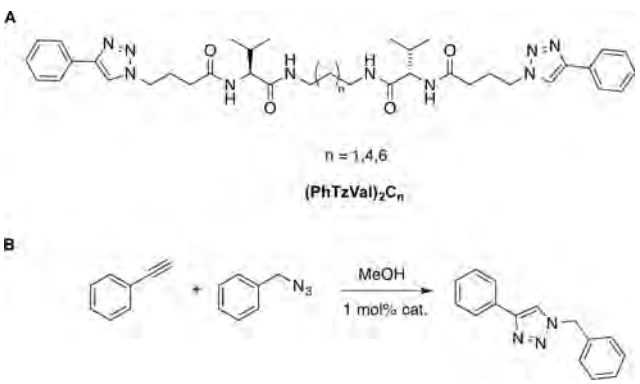

Scheme 17. A) Structure of gelator ligand and **B)** schematic representation of azide-alkyne click reaction.

Catalysis in metallogels

Reactions carried out in presence of metal catalysts can be also performed in gels. In this case, the metallogels can be formed upon interaction or complexation of a suitable ligand to a metal ion, and the presence of this latter is necessary for the gel to form. While, in other cases, metallogels can be formed by doping a suitable gel with a metal salt or complex.

For example, Escuder *et al.* employed metallogels formed in methanol by L-valine derived gelators **$(PhTzVal)_2C_n$**, functionalized with triazolyl moieties in the presence of Cu(I), as heterogeneous catalyst for the azide-alkyne cycloaddition between phenylacetylene and benzylazide, as well as for the autocatalytic synthesis of the gelator itself (Scheme 17A).[28]

The reaction performed in the presence of the gels afforded higher conversion and yields compared with the ones obtained in the presence of the Cu(I) salt $[Cu(CH_3CN)]PF_6$. This was attributed to the stabilization of the oxidation state of Cu(I) imparted by the coordinating triazole moieties, together with the proximity of catalytic sites within the gel fibers. Studying the synthesis of the gelator catalyzed by the same gels, evidenced that the catalytic efficiency was influenced by the 3D-arrangement of the gel network. Wide angle X-ray diffraction analysis (WAXD) suggested that gels having lower short-range order exhibit better catalytic performance.

On the grounds of this study, hydrogels formed by the L-valine gelator, with n = 3 and in presence of Cu(I), **Cu(I)-$(PhTzVal)_2C_3$**, were also used to perform the tandem aldol-click reaction between phenylacetylene, *p*-nitrobenzaldehyde, and an azide containing a ketone moiety, Scheme 18.[29]

In addition to the final products, the formation of the intermediate products 4.syn and 4.anti or 6 was observed in dependence on the competitiveness of the three-component reaction system (Scheme 19). These intermediate products further underwent 'click' or aldol addition, yielding the final reaction products.

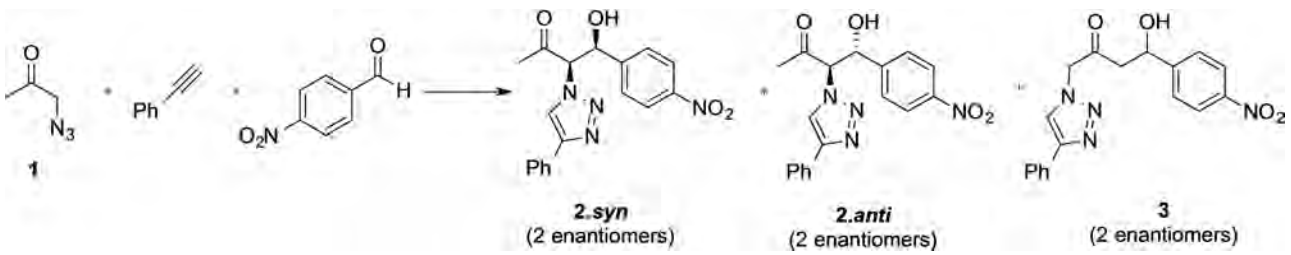

Scheme 18. Schematic representation of the aldol- click reaction performed in hydrogels.

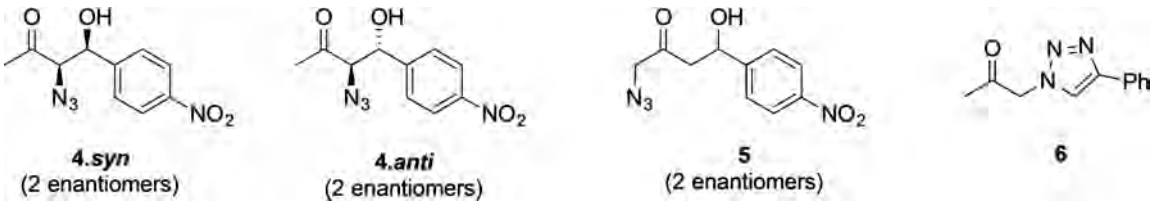

Scheme 19. Possible additional products of the aldol-click reaction performed in hydrogels.

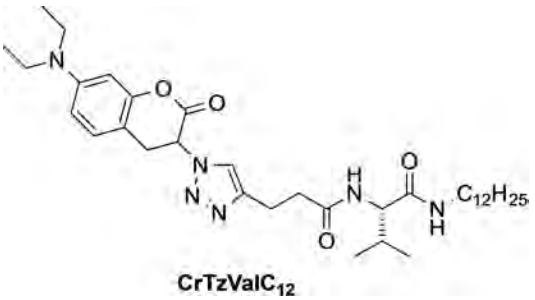

Scheme 20. Structure of **CrTzValC$_{12}$** gelator ligand used for the azide-alkyne click reaction.

Compared to the reaction performed in presence of pure **(PhTzVal)$_2$C$_3$** aggregates, CuBr or only in water, the metallogel **Cu(I)-(PhTzVal)$_2$C$_3$** showed the best catalytic efficiency for both 'click' and aldol reactions, reaching in 4 days 97% and 30% conversions for products 6 and 2.syn, respectively.

In addition, authors demonstrated that simply adjusting the amounts of reactants, with 10 mol% of metallogel **Cu(I)-(PhTzVal)$_2$C$_3$**, conversions of around 65% in two days were achieved.

The proposed mechanism of the catalysis of the aldol addition in the presence of the metallogel **Cu(I)-(PhTzVal)$_2$C$_3$** followed a type II aldolase mechanistic pathway, where the coordination of the substrate to the metal center resulted in the polarization of the carbonyl group and consequent acidification of the α-hydrogen, whose removal might be assisted by an increase in the basicity of the medium provided by the supramolecular gelation of the catalyst.

This biomimetic catalytic activity shown by the metallogel **Cu(I)-(PhTzVal)$_2$C$_3$** has been observed for the first time, opening a new insight on the application of triazole functionalized compounds for the tandem catalysis of 'click'-aldol multi-component systems.

The same authors also studied the catalytic ability of Cu(I) metallogels formed by L-valine amphiphilic gelator, **CrTzValC$_{12}$**, with only one triazole functionality (Scheme 20), for the same Huisgen 1,3 dipolar cycloaddition between phenylacetylene and benzylazide reported in Scheme 17.[30]

Interestingly, in this case, the addition of benzylazide and phenylacetylene to the reaction medium promoted the disassembly of the gel. Nevertheless, the dynamic behaviour of this system provided a good catalytic activity to the gel obtaining conversions of 71% in 3 hours, in the presence of 1 mol% of catalyst. Furthermore, the system could be continuously reused for three consecutive runs without losing its catalytic activity. In comparison with **(PhTzVal)$_2$C$_3$**-based metallogels, in this case, the main novelty is that the non-equilibrium behaviour of the metallogel can be regulated by the model 'click' reaction.

Click reactions with several reactants were recently carried out also in supramolecular gels formed by glycoclusters with three, four, and six arms of glycosyl triazoles in presence of $CuSO_4$ (Scheme 21). The metallogels were, once again, more efficient than the corresponding solutions and in addition, they

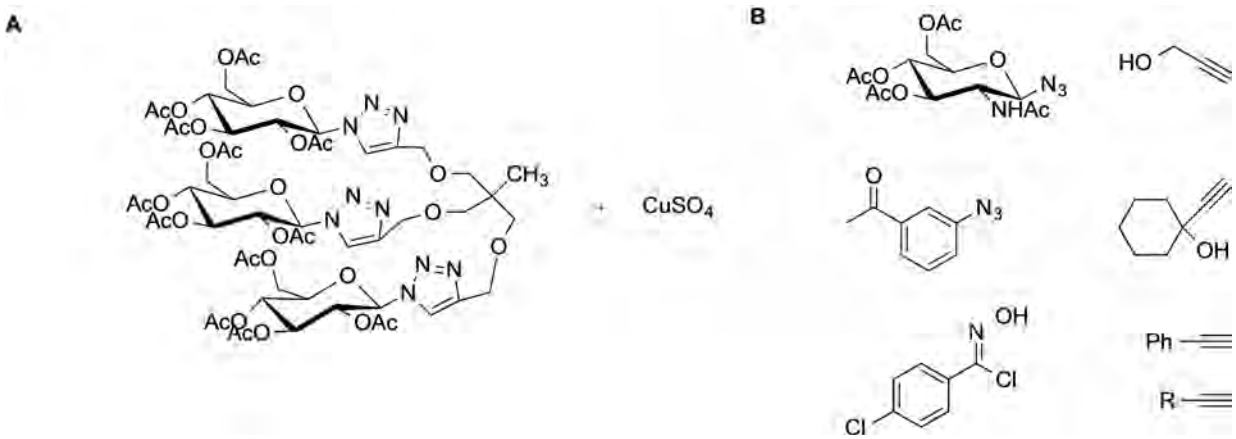

Scheme 21. A) Structure of glycocluster gelator, **B)** schematic representation of click reactants used.

could be prepared as gel columns, which could be reused for cycloaddition reactions several times. In particular, the glucose derivative gels were especially effective for the phenylacetylene click reaction and were used for the synthesis of several triazoles and isoxazoles.[31]

Cu(II) based metallogels were also applied as reaction media for Diels-Alder cycloaddition between cyclopentadiene and azachalcone (Scheme 22).[14c] In particular, it was demonstrated that the introduction of Cu(II) into a glutamic acid-based bolaamphiphilic lipid caused the formation of supramolecular nanotubes with a multilayer wall. Such nanotubes showed enhanced catalytic behavior and accelerated the asymmetric Diels-Alder cycloaddition in comparison with other nanostructures containing Cu(II). Probably, the alignment of the catalytic sites on nanotube's surface and the stereochemical environment enhanced the enantioselectivity of the system.

Cu(II)-doped organogels formed by a urea-based gelator, were also applied as catalyst for the oxidation of a sulfur mustard compound. Sulfur mustards are vesicant halogenated sulfide species used as chemical warfare. A strategy for the decontamination of soils and the neutralization of such compounds consists in their oxidation to sulfoxides. Hence, Hiscock *et al.* employed an organogel of bis-urea doped, ***trans*-Cy(UC$_{12}$)$_2$**, with a complex of copper (II) hexafluoroacetylacetonate, Cu(hfac)$_2$, for the oxidation of a sulfur mustard model compound (Scheme 23), in the presence of *tert*-butyl peroxide (*t*-BuOOH).[32]

Carrying out the oxidation within the gel phase proved convenient over conventional solution phase reaction since reactants and products are confined in a solid-like matrix, thus minimizing contamination by leakage or evaporation. Moreover, this catalytic system afforded selectively the sulfoxide, avoiding over-oxidation to the relevant sulfone compound, which is undesirable, since these compounds are also vesicants.

Another application of a gel as heterogenous catalyst was described by Banerjee *et al.*[33] In this case, a two-component hydrogel formed by graphene oxide and tris(aminoethyl)amine, was reduced *in situ* by ascorbic acid, leading to a gel-to-gel conversion, resulting in a hydrogel formed by reduced graphene oxide and polyamine. This gel was finally able to entrap and stabilize gold nanoparticles (AuNP), forming a hybrid hydrogel. This latter was used as catalyst for the reduction of *p*-nitrophenol and *p*-nitroaniline to *p*-aminophenol and p-phenylenediamine in the presence of $NaBH_4$. The hybrid gel allowed the reaction to go to completeness within 5 minutes, could be easily separated from the reaction mixture and recycled four times without reduction in catalytic performance.

Dastidar *et al.* described the use of metallogels based on tripodal pyridyl-functionalized ligands in the presence of Ag^{I} salts. The gels were composed by coordination polymers of the ligands and silver cations, with the ligands chosen on the basis of crystal engineering considerations (Scheme 24).[34]

Upon exposure to UV or visible light, reduction of silver cations to Ag occurred, presumably by the ligands themselves, resulting in formation of silver nanoparticles (AgNPs). Hence, the AgNPs-containing metallogels were effective in promoting the reduction of *p*-nitrophenolate to *p*-aminophenolate, without the need for any external reducing agent.

A different type of gels is constituted by double-network gels, comprising both supramolecular gel network and a polymeric one, within the same gel phase. The polymer gel matrix imparts toughness and mechanical robustness to the whole material, thus reinforcing the mechanical properties of the supramolecular gel. An example of such gels with catalytic applications was reported by Smith *et al.*[35] In particular, they employed double-network hydrogels formed by a supramolecular gelator derived from 1,3 : 2,4-dibezylidenosorbitol (**DBS-CONHNH$_2$**) and agarose as polymeric one (Scheme 25A).

These hydrogels were used to scavenge Pd(II) from solutions, leaving a residual palladium concentration far below

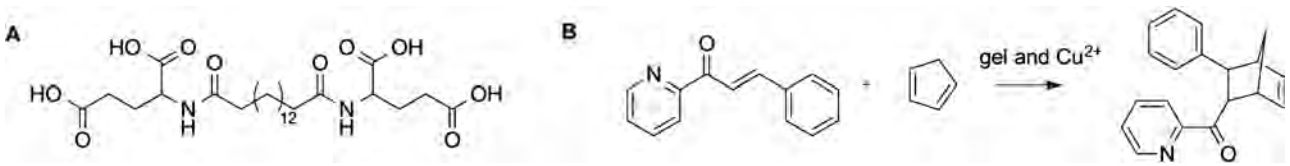

Scheme 22. A) Structure of glutamic acid derived gelator, **B)** schematic representation of Diels-Alder reaction.

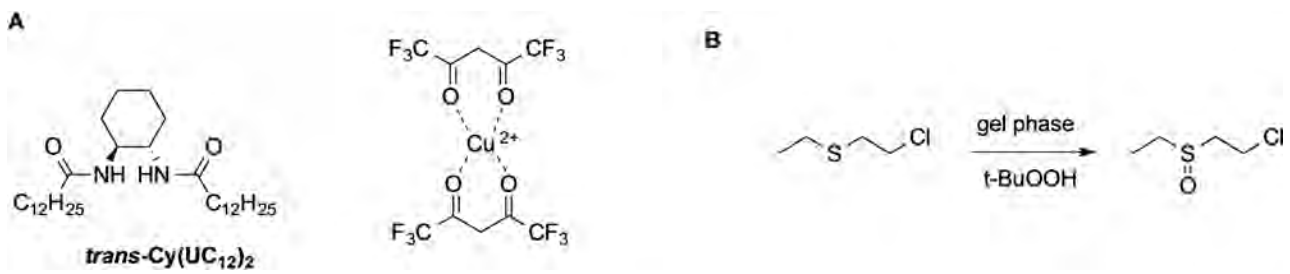

Scheme 23. A) Structure of organogelator and Cu(II) complex, **B)** schematic representation of oxidation of model sulfur mustard compound.

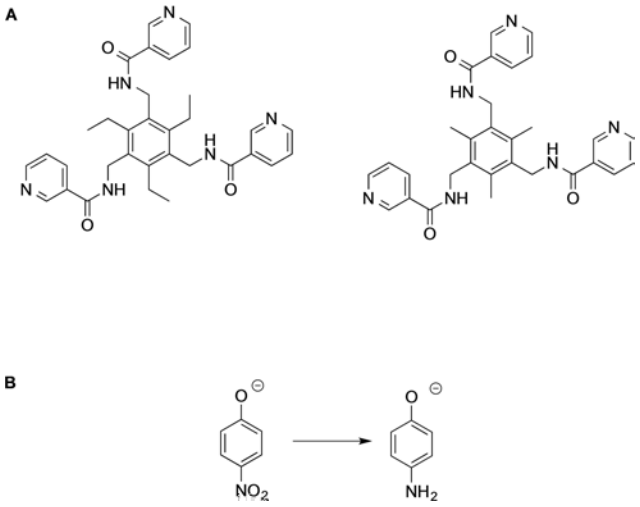

Scheme 24. A) Structure of gelator ligands and **B)** schematic representation of *p*-nitrophenate reduction.

the levels recommended in the pharmaceutical industry. Since **DBS-CONHNH$_2$** can reduce Pd(II), in situ reduction of Pd(II) to Pd occurred with formation of palladium nanoparticles, giving rise to hybrid, metal containing gels. These latter could be used as catalyst for the Suzuki-Miyuara cross coupling between phenylboronic acid and a wide range of aryl iodides. The reaction afforded high yields (86 and 90%) and the gel could be recycled ten times with no loss in performance, with a very limited leaching. On a similar note, the same group reported the catalytic application of hybrid, PdNPs containing double network hydrogels comprising **DBS-CONHNH$_2$** and alginic acid. In this case, the double-network gels were prepared as core-shell gel beads by adding dropwise the hot solution containing alginic acid and **DBS-CONHNH$_2$** to an aqueous solution of $CaCl_2$ (Scheme 25B).[36] Since **DBS-CONHNH$_2$** can reduce Pd(II), the hybrid gel beads were contacted with a solution of $PdCl_2$ inducing *in situ* reduction to Pd and entrapment of palladium nanoparticles (PdNPs) within the gel matrix, as confirmed by TEM and SEM. These hybrid gel-beads were used as catalysts of the aforementioned Suzuki-Miyuara coupling (Scheme 25C), with high yields and conversions (>98%). Moreover, the same gel bead could be reused at least five times without loss in performance, although some metal leaching into the reacting mixture was detected.

In addition, these **DBS-CONHNH$_2$**/agarose hybrid hydrogels with embedded PdNPs can catalyse copper-, amine-, and phosphine-free Sonogashira cross-coupling without the need for inert conditions and using green solvents such as EtOH/H_2O or PEG 200.[37] These catalysts were recycled up to five times with no adverse impact on yield. The PdNP-loaded gel catalysts compared with the dried xerogel form showed better performances in terms of selectivity and recycling ability, even if xerogels could be used at higher temperatures.

Good activity of PdNP hybrid hydrogels was observed also for the Heck cross-coupling reaction, using milder and environmentally-friendly conditions compared with usual Heck reaction conditions. Importantly, these catalysts can be generated very simply by exposing the gel to Pd(II) waste, with the added benefit of cleansing the waste stream.

The catalytic properties of Pd-based metallogels were also reported for some alginate ionogels (Pd-Alg_ionogels), using the allylic substitution of (E)-1,3-diphenylallyl acetate with morpholine as model reaction (Scheme 26).[38] Pd-Alg_ionogels allowed to obtain good yields (93%) at room temperature in 1.5 h. Recycling tests showed that the Pd-Alg_ionogels could be

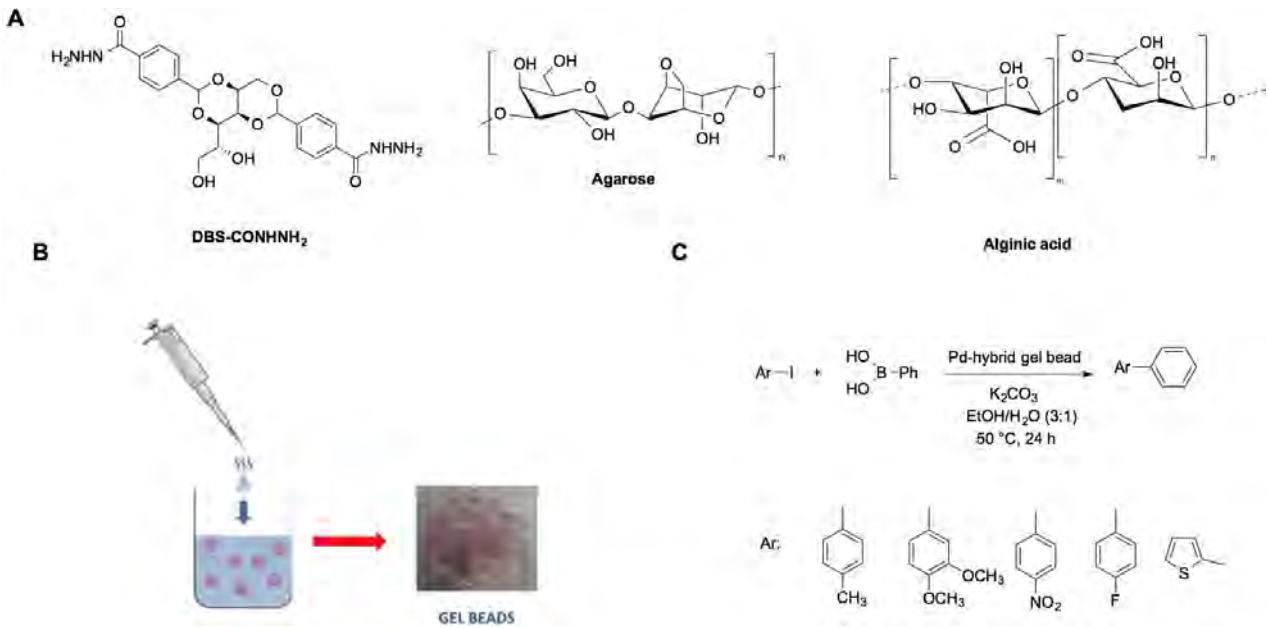

Scheme 25. A) Structure of supramolecular and polymeric gelators, **B)** pictorial representation of the preparation of gel beads; reproduced from Ref. [36]. **C)** Schematic representation of Suzuki-Miyuara reactions.

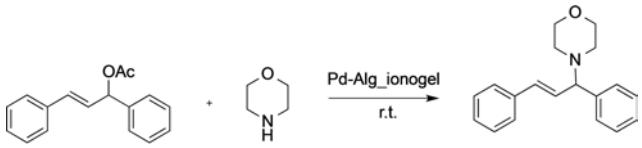

Scheme 26. Schematic representation of Tsuji-Trost reactions.

successfully reused up to 7 times. However, a decrease in activity was observed in the fourth run. This was attributed either to a leaching phenomenon of the catalyst during the extraction step and to a deactivation of the catalyst. In particular, it was demonstrated that the deactivation of the catalytic material is not only related to the aggregation of Pd-based particles, but also to a partial decomplexation of the phosphorus ligand in the catalyst.

Basic ionic liquid gels were, also, used as reaction media for the hydrogen transfer dehydration of 1,3-propanediol to propanal, catalyzed by Ir complexes (Scheme 27). Gels comprising a mixture of basic and hydrophobic ionic liquids, such as $[P_{6,6,6,14}][OH]$ and $[C_2mmim][NTf_2]$, gave the best results. The catalytic system exhibited excellent conversion, selectivity and good recyclability. Nevertheless, the main advantage was that the reaction proceeded in the ionic liquid gel enabling the continuous removal of propanal under reduced pressure.[39]

Moreover, macroporous hydrogels based on a modified protein were shown effective in the encapsulation and stabilization of AuNPs. In particular, Diaz-Diaz *et al.* reported the preparation of a macroporous hybrid gel made of a modified apoferritin embedding AuNPs.[40] To this aim, native ferritin was first covalently modified, which then self-assembled in the presence of a surfactant and cross-linker. The protein was then stripped of its iron oxide core, which was substituted by AuNPs by soaking the hydrogel with a $HAuCl_4$ solution containing $NaBH_4$ (Scheme 28).

The macroporous gel obtained was used as catalyst for a nitroaldol reaction and the reduction of nitroarenes, in water at room temperature. For the nitroaldol reaction, the hybrid gel was mostly effective in the presence of strong electron withdrawing substituents in the aldehyde, whereas yields were less satisfactory in other cases. For the nitroarene reduction, the reaction occurred faster than other commonly used catalysts based on zero-valent Ag- and Au nanoparticles.

Metallogels have also shown enzyme like activity. In this regard, a metallogel formed by vanadate complex with a

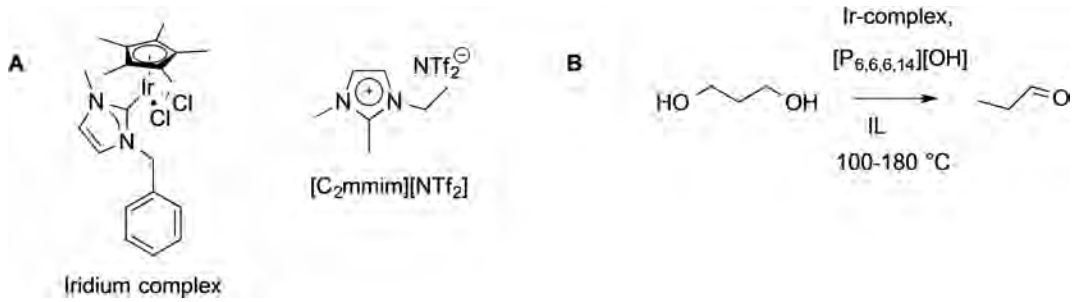

Scheme 27. A) Structures of Iridium complex and IL used, **B)** schematic representation of Dehydration of 1-propanediol, in based ionic liquid gels.

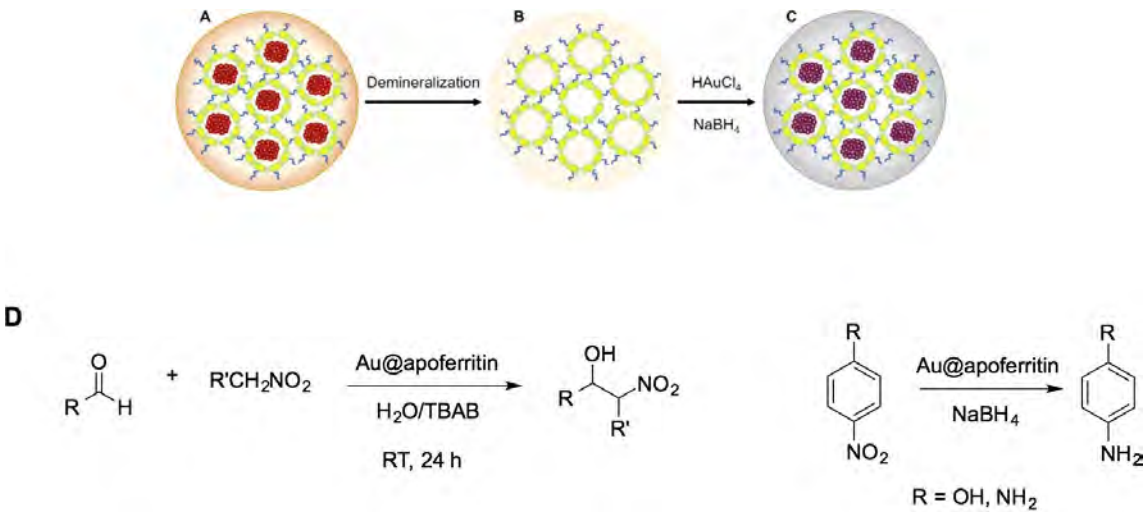

Scheme 28. A), B), C) Pictorial representation of the replacement of iron oxide core in the macroporous hydrogel with AuNPs. Reproduced from Ref. [40]. **D)** Schematic representation of reactions catalyzed by hybrid macroporous gel.

hydrazonic ligand (VO_2-L, Scheme 29) was used as catalyst for the oxidative bromination of organic substrates such as aromatic alcohols and ketones, in the presence of H_2O_2, thus mimicking a bromoperoxydase behavior.[41]

The metallogel, formed in water:methanol (9:1, v:v) promoted the oxidative bromination, affording yields higher than the ones observed in the presence of the neat gelator, or other vanadium containing species like $VOSO_4$, V_2O_5 or $NaVO_4$.

Photocatalysis

Photon upconversion based on triplet-triplet annihilation (TTA-UC) is a photochemical technique applied in photocatalysis[42,14e,43] that converts low-energy into high energy levels between a donor and an acceptor molecule, generating delayed upconverted fluorescence. This technique can be also efficiently applied in supramolecular gels.

For example, this technique was applied by Duan *et al.* In particular, supramolecular organogel nanofibers were used as matrices to confine sensitizer and emitter molecules providing air-stable UC gels via solvophobic interactions (Scheme 30).[44] *N,N'*-bis(octadecyl)-L-boc-glutamic diamide (**LBG**) was the gelator able to form pink supramolecular gels in DMF. The TTA-UC system was obtained adding to the gel Pt(II) octaethylporphyrin (PtOEP) as donor molecule and 9,10-diphenylanthracene (DPA) as acceptor molecule. It was observed that UC phenomenon is particularly stable in gel phase, remaining almost unchanged even under exposure to air for 25 days. Conversely, an opposite situation was observed in DMF solution, as the UC emission intensity rapidly decreased in the presence of air.

Diaz Diaz and coworkers[45] used the previous acceptor/donor TTA system (PtOEP/DPA) to perform the intragel photoreduction of aryl halides by green to blue UC at mild conditions (room temperature and aerobic atmosphere), that are inapplicable in solution media. In addition to the same gel system reported in Scheme 30 (**LBG**/DMF), they used also a gel formed by (*1S,2S*)-cyclohexane-1,2-diyl)didodecanamide as gelator, **trans-Cy(UC_{11})$_2$**. Both gel systems implemented with donor and acceptor molecules were applied to perform the photoreduction of *p*-bromoacetophenone in acetophenone (Scheme 31).

The reaction proceeds with good mass balance, yield and conversion when the LBG gel was used as medium, in comparison with the same reaction carried out in DMF solution (6%, 96%, 2% in DMF solution *vs.* 65%, 98%, 58% in **LBG**-gel, for conversion, mass balance and yield, respectively). Similar results were achieved using the gel formed by ***trans*-Cy(UC_{11})$_2$** gelator. TTA system was stable under these conditions affording the photoreduction product without formation of by-products. Moreover, no significant improvement in reaction outcomes were observed under nitrogen atmosphere, confirming the efficiency of gel system in aerobic condition.

They also investigated some photoinduced C–C cross-coupling reactions under aerobic conditions into gel phase, performing functionalisation of aryl halides.[46] In this case, the gel system was composed by the Rh-6G as photocatalyst, *N,N*-diisopropylethylamine (DIPEA) as electron donor, a proper gelator and DMSO as solvent (Scheme 32). They used four different gelators, in addition to **LBG** and ***trans*-Cy(UC_{11})$_2$** reported in Scheme 30 and 31, ***trans*-Cy(UC_{12})$_2$** and 1,3:2,4-bis(3,4-dimethylbenzylidine)-sorbitol were also employed.

The reaction strategy involved the generation of the excited Rh-6G$^{\bullet -*}$ radical anion in the presence of DIPEA upon blue-light irradiation (455 nm). In solution of DMSO, these reactions required nitrogen atmosphere, due to the susceptibility of the Rh-6G radical to the oxygen. However, when reactions were carried out into gel, this limitation was overcome. The yields for

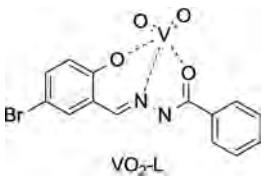

Scheme 29. Structure of vanadate complex gelator.

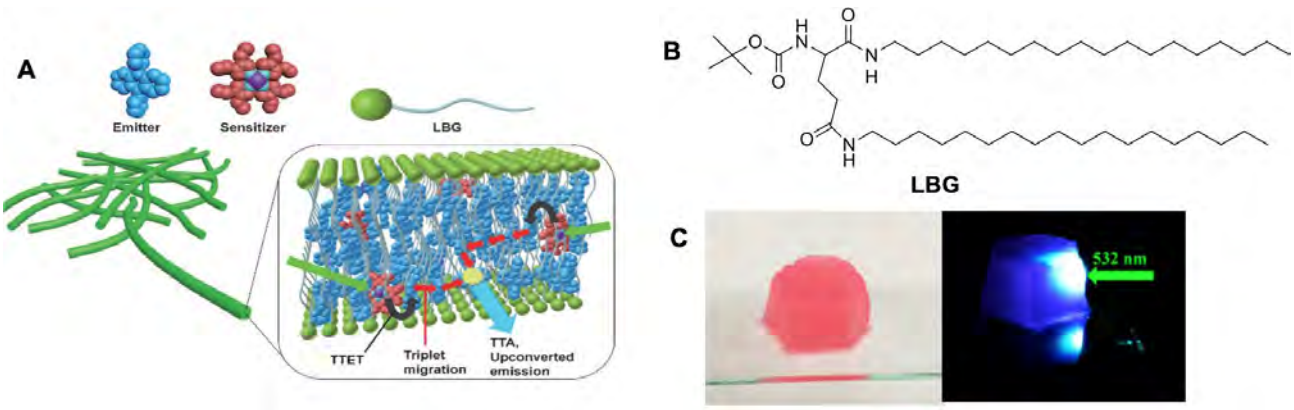

Scheme 30. A) Schematic representation of the unit structure of upconversion gel system. Donor (red) and acceptor (blue) molecules are incorporated in the *N,N'*-bis(octadecyl)-L-boc-glutamic diamide (LBG) nanofibers as extended domains. **B)** *N,N'*-bis(octadecyl)-L-boc-glutamic diamide (LBG) structure; **C)** white light and 532 nm green laser ([PtOEP] = 33 μM, [DPA] = 6.7 mM, [LBG] = 13.3 mM). Reproduced from Ref. [44], Copyright (2015), with permission from American Chemical Society.

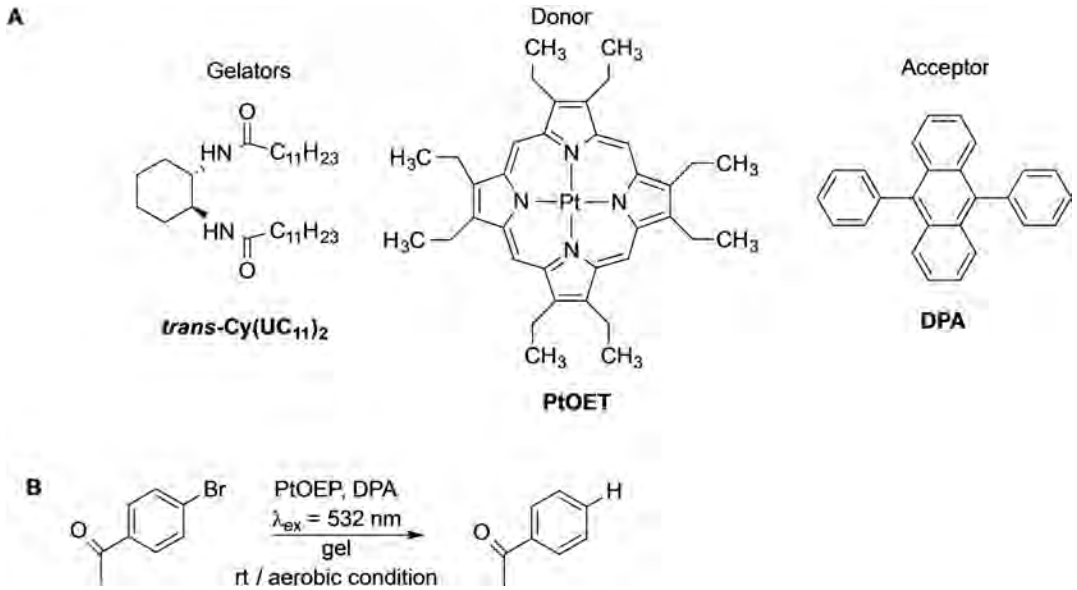

Scheme 31. A) Structures of gelator and photocatalytic system; **B)** schematic representation of photoreduction of *p*-bromoacetophenone in acetophenone.

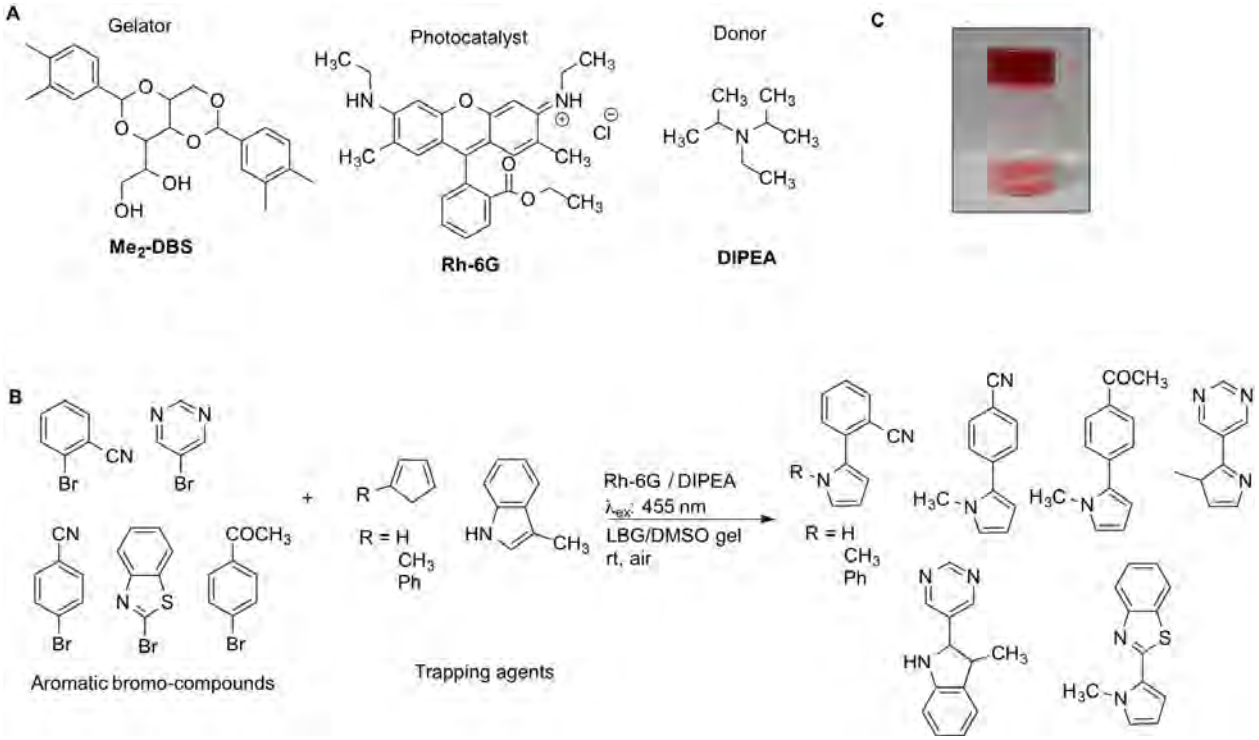

Scheme 32. A) Structure of gelator, photocatalyst and donor; **B)** schematic representation of photoredox catalytic arylation by one-to-one combination of bromo-compounds and trapping agents; **C)** gel doped with reactants. Picture reproduced from Ref. [46], Copyright (2018), with permission from American Chemical Society.

the intragel arylation reported in Scheme 32 varied between 32 and 78%, depending on the substrate and the compound considered. In general, with all gelators considered, comparable yields were obtained.

The same group reported the selective activation of Rh-6G depending on irradiation wavelength using the same gelled photocatalytic system used for reactions in Scheme 32 (Scheme 33).

The coupling between 1,4-dibromo-2,5-difluorobenzene and *N*-methylpyrrole led to the corresponding monosubstituted product or disubstituted one with green LED light (530 nm) and blue light (455 nm), respectively. In the latter case, the reaction

proceeds through the generation of excited Rh-6G$^{\bullet -*}$ radical anion. While, in the case of irradiation at 530 nm a ground-state Rh-6G$^{\bullet -}$ radical anion is involved.

The same photocatalytic system was also employed for a sequential substitution (Scheme 34) varying the order of irradiation wavelength.

The low reactivity of the diphenyl compound toward nucleophiles and electrophiles was overcome by performing the reaction inside the gelatinous matrix, obtaining the final product in good yield (60%). It is important to note that the supramolecular network allowed an easy separation of desired products and the reuse of the gelator not compromising the gelation ability.

Recently, also the photolysis of heteroarene with bis-(pinacolato)diboron (B_2pin_2) and DIPEA was carried out in **LBG** and ***trans*-Cy(UC$_{11}$)$_2$**-based organogels in aerated conditions (Scheme 35).[47] Interestingly, once again, the same reaction performed in aerated solution did not give rise to any product. In addition, the visible-light-driven thiophene borylation, firstly carried out as model reaction to set all reaction conditions, was considerably improved in the gel network in respect to the one performed in solution under inert atmosphere.

Both gelators achieved good yields, underlining the role of the viscoelastic gel matrix as efficient nanoreactor. In particular, in addition to a kinetic effect exerted by the gel, it was demonstrated that the reactants were not only localized in the solvent pools between fibers, but they could also spread through fibers, permitting photochemical reaction in a confined by dynamic space. Finally, the gel network provided an adequate stabilizing microenvironment to support wide substrate scope, spanning from furan, thiophene, selenophene, and pyrrole boronate esters. This easy and efficient synthetic strategy, thus, allows to obtain heteroarene boronate esters that constitute valuable building blocks to prepare new heteroarene bioactive molecules.

Polyamide-based supramolecular gels were also applied as reaction media to carry out air-sensitive and metal-free, light-induced trifluoromethylation of six-membered (hetero)arenes

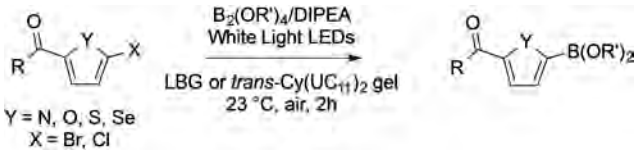

Scheme 35. Schematic representation of visible light-driven borylation of heteroarenes in gel media under aerobic conditions.

under aerobic conditions (Scheme 36).[48] The reaction was performed at room temperature using sodium triflinate as a source of radicals and diacetyl as electron donor. It was observed that different variables influenced the yields and selectivity of the reaction, especially the type of gelator and its concentration. For example, the diprotected-Fmoc-lysine derived gels were more selective but less reactive than **LBG**, ***trans*-Cy(UC$_{12}$)$_2$** and 1,1′-(4-methyl-1,3-phenylene)bis(3-(2-ethylhexyl) urea), **C$_1$Ph(C$_2$C$_6$U)$_2$** ones (Scheme 36A). In most cases, under comparable conditions, the reaction with different substrates performed in aerated gels afforded the desired products in higher yields than in degassed solutions. The results confirmed the blocking effect of the gel medium against reaction quenching by external oxygen, as well as a certain control on the kinetics and selectivity.

Yang *et al.* reported also multi-component LBG-based supramolecular gels and two types of free base porphyrins, 5,10,15,20-tetrakis(4-(hydroxyl)-phenyl)porphyrin (THPP) and 5,10,15,20-tetrakis(4-(carboxyl)-phenyl)porphyrin (TCPP) for the photocatalytic hydrogen production (Scheme 37).[49] The two porphyrins formed exciplexes and were protonated under neutral conditions upon gelation (Scheme 37C). Protonation and *J*-aggregation of porphyrins, led to a broader UV-visible absorption.

In dependence on the gelation solvents, DMF or ethanol, the gel properties could be modulated, and the best performance were obtained in DMF. Addition of Pt allowed performing the reaction of H_2 generation. Using ascorbic acid as the

Scheme 33. Chromoselective 1- or 2-fold substitution reaction between 1,4-dibromo-2,5-difluorobenzene and *N*-methylpyrrole. Photocatalytic system is reported in Scheme 32.

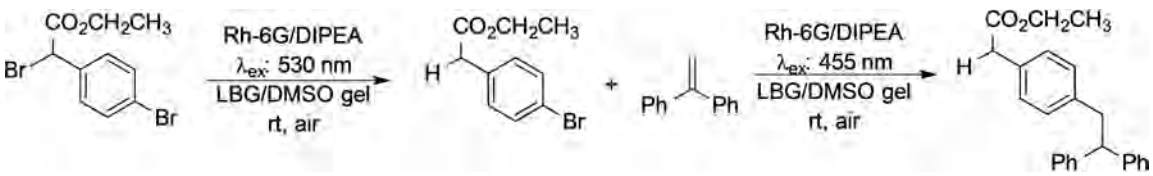

Scheme 34. Sequential photocatalytic reaction of ethyl 2-bromo-(4-bromophenyl)acetate with 1,1-diphenylethylene. Photocatalytic system is reported in Scheme 32.

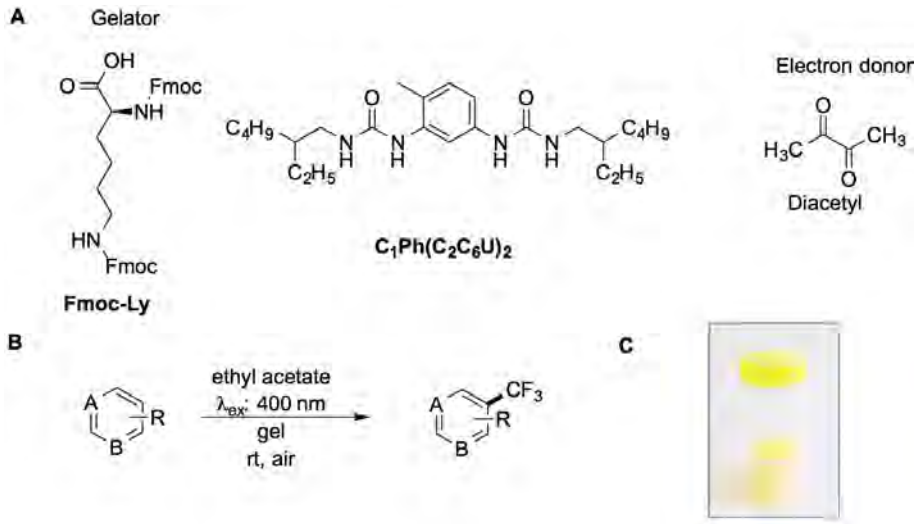

Scheme 36. A) Gelator and electron donor structure; **B)** reaction scheme for trifluoromethylation; **C)** gel doped with reactants. Picture reproduced from Ref. [48], Creative Commons Attribution License, with permission from MDPI.

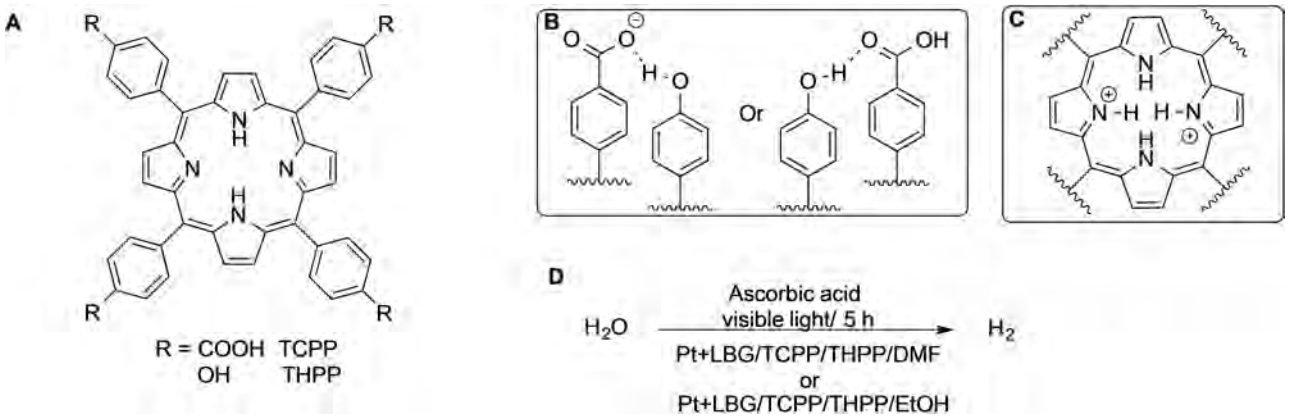

Scheme 37. A) Structures of porphyrins; **B)** interaction between porphyrin units; **C)** sites of porphyrin protonation; **D)** photocatalytic production of H_2 from water using ascorbic acid as sacrificial reagent and visible-light as irradiation source.

sacrificial reagent, the amount of H_2 after 5 h, under visible light irradiation, obtained within the DMF-gel was seven times higher than the amount generated within EtOH-gel system. In addition, the amount of H_2 generated in DMF gel was fifteen times higher than the one obtained using the simple gel system with only one porphyrin (LBG/TCPP/Pt). Moreover, gel systems could be recycled several times demonstrating the stability of supramolecular gels in photocatalysis.

Liao *et al.* designed similar gel system based on porphyrin to perform visible-light-induced H_2 generation, using sodium ascorbate as sacrificial electron donor in the presence of Pt as the proton reduction catalyst.[50] In the gelled systems the photocatalytic active species were structural part of the gel, showing high stability and high photocatalytic H_2 generation from water by visible-light irradiation.

On the other hand, Stupp and co-workers took advantage of perylene monoimide (PMI) properties to design supramolecular hydrogels for H_2 generation (Scheme 38).[51] Chromophore amphiphiles (CAs) containing PMI and carboxylate groups assembled into ribbon-shaped nanostructures in water, varying the assembly morphologies in dependence on the length of the linker. The PMI systems with linker length up to 7 units in aqueous solutions showed highly blue-shifted absorbance, consistent with strong electronic coupling within *H*-aggregates.

For H_2 generation, the best results were achieved with PMI with linker length of 5 (L5) and 7 (L7). However, L5 photosensitized more than L7, due to the smaller distance between the PMI core and catalyst. The reaction proceeded with the formation of PMI radical anion, which reduced twice the Nickel catalyst, as a key step of the H_2 production.

Ajayaghosh and co-workers investigated how supramolecular network assembly of the gel can induce the formation of photoproducts and how these systems can be applied in photonic devices.[52] For example, 9-phenylethylanthracene derivative was able to assembly in methyl cyclohexane

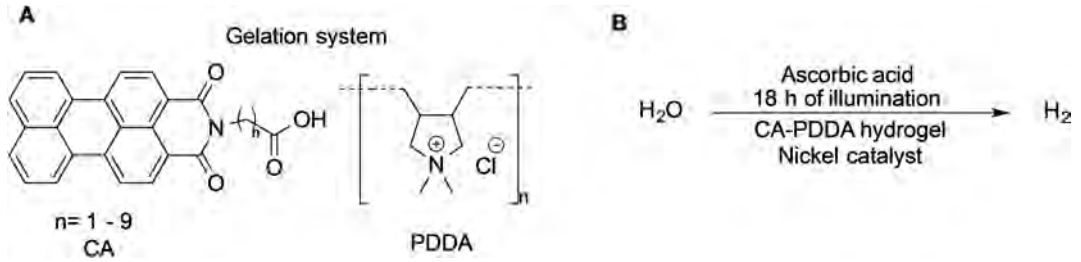

Scheme 38. A) Perylene monoimide compound and poly-diallyldimethylammonium chloride; **B)** photocatalytic production of H_2 from water using ascorbic acid as sacrificial reagent and an irradiation source.

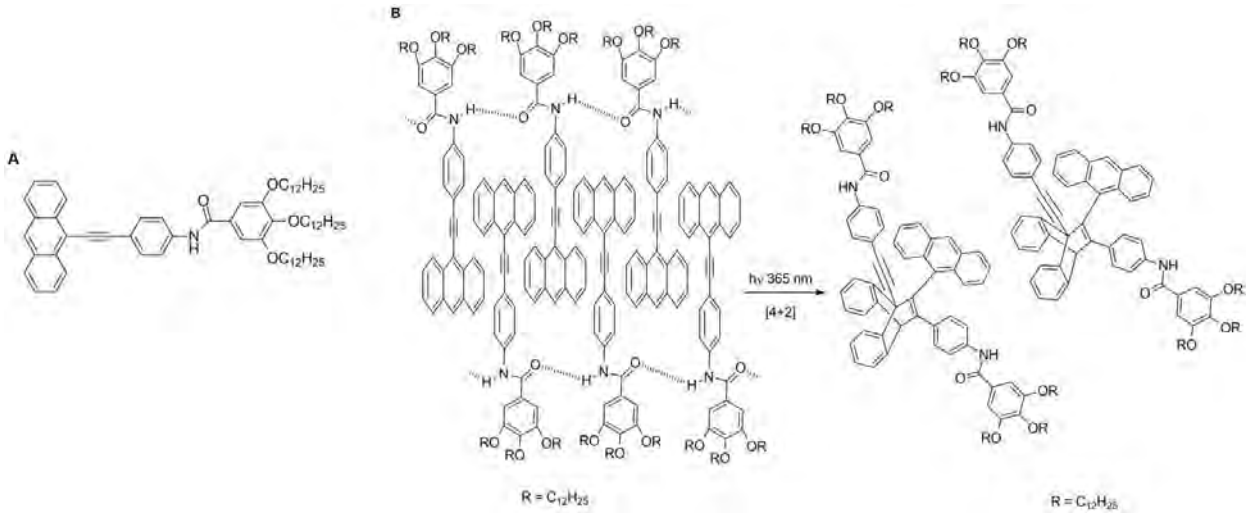

Scheme 39. A) Structure of 9-phenylethylanthracene derivative; **B)** molecular assembly and structural change of 9-phenylethylanthracene derivative before and after photoirradiation.

(Scheme 39). The gel phase generated the ideal confinement for the specific [4 + 2] Diels-Alder photoreaction by irradiation of the gel at 365 nm. The devices formed by the 9-phenylethylanthracene derivative exhibited a blue emission, whereas the device based on the photoproduct showed white electroluminescence.

Moreover, Bath and Maitra studied the effect of supramolecular hydrogel on selectivity of dimer ratio in the photoinduced dimerization process of acenaphthylene (Scheme 40).[53] The ratio of *anti* to *syn* photodimers was found to be greater in hydrogel formed by bile derivative and its derived salts than in solution, determining dimer ratios between 3.5 and 11. Selectivity of the product was shown to correlate with the stiffness of the gels.

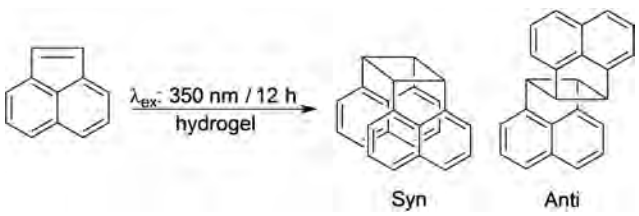

Scheme 40. Schematic representation of photodimerization reaction of acenaphthylene.

Shinkai *et al.* took advantage of supramolecular gel system also to improve the control on dimerisation stereochemistry.[54] A photoresponsive organogel formed by a gelator containing 2-anthracenecarboxylic acid non-covalently attached with another gelator component containing the gallic acid backbone coupled with D-alanine, was used to perform the stereoselective dimerization. The head-to-head photocyclodimers were exclusively obtained with significant enantiomeric excess induced by the chiral counterpart of the gelator.

Bachl *et al.* investigated how the involvement of the catalyst in the organisation of gel network can influence a photocatalyzed reaction. Riboflavin tetraacetate catalysed aerobic photooxidation of 1-(4-methoxyphenyl)ethanol reaction under blue visible light (440 nm) in different gels under aerobic conditions (Scheme 41).[55] In details, the photocatalyst can be physically entrapped into the self-assembled gel matrices, or can be covalently attached to a gelator structure. Finally, the photocatalyst can be also supramolecularly assembled with another molecule forming the gel phase. Low-molecular-weight (LMW) and biopolymer-based gelators were used to this aim.

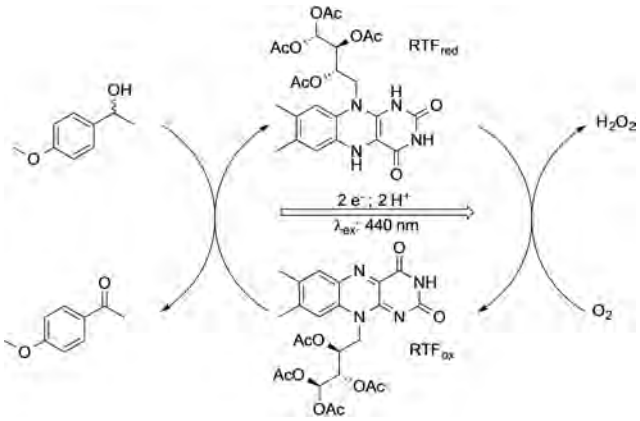

Scheme 41. Flavin-derivatives (RFT) mediated photooxidation of benzyl alcohols under visible blue light irradiation.

In general, the degree of organisation of the catalyst was correlated to the outcomes of the reaction. In the case of physical entrapment of the catalyst and the substrate into hydrogels, the reaction conversions were between 55 and 100% within 120 min. Conversely, when the catalyst acted as gelator, slower reaction rates were observed.

Biocatalysis in gel

Obtaining supramolecular gels with precise structural organization and catalytic ability often requires lots of efforts and is still challenging. The combination of biocatalysis and molecular self-assembly, opens a new pathway to easily access higher-ordered structures.

For example, it has been demonstrated that, by simply increasing enzyme concentration, supramolecular order can be drastically enhanced, without any increase in the gelator concentrations. In particular, amphiphile molecules were prepared by attaching an aromatic moiety to a dipeptide backbone capped with a methyl ester. Their self-assembly was induced by a hydrolytic enzyme from *Bacillus licheniformis*, which hydrolyses the methyl ester to form a peptide derivative that self-assembles (Scheme 42).[56] The same result was obtained using the biocatalytic action of phosphatases on Fmoc-protected dipeptide.[57]

In addition, to allow supramolecular gel self-assembly, biocatalysis can be also carried out in gels adding the enzyme on preformed gels. For example, some supramolecular gels were used as vessels for the action of glutathione peroxidase

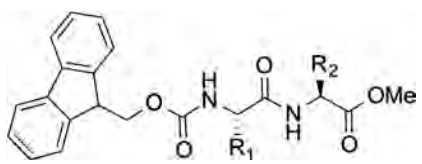

Scheme 42. Structure of gelator molecules.

(GPx), that protects cells from oxidative damage by scavenging surplus reactive oxygen species (ROS). These supramolecular gels were formed by host-guest interactions among guest molecules containing tellurium and host molecules formed by cyclodextrins functionalized with some copolymers (Scheme 43). The catalytic behaviour of the system was evaluated studying the reduction of cumene hydro-peroxide (CUOOH) by TNB (3-carboxyl-4-nitrobenzenethiol), demonstrating enhanced efficiency. Furthermore, the catalytic rate exhibited a temperature responsive behavior, probably thanks to the changes of the hydrophobic microenvironment and the pore size in gel network.[58] The gel was further employed using a tellurium crosslinked polymer as guest molecule of the cyclodextrin. This modification brought to a drastic increase of catalytic activity and of temperature responsive behavior.[59]

Supramolecular organogels formed by crown ethers appended to chiral bis-urea supergelator were able to trap enzymes and release them on demand by chemical stimuli (Scheme 44). The gel can stabilize the microparticles in Pickering emulsions so that enzyme-catalyzed organic reactions can take place in the polar phase inside the microparticles. In particular, a lipase derived from *Candida Antarctica* was used as enzyme, while the esterification between 1-octanol and octanoic acid was chosen as model reaction.[60] It was observed that enzyme activity in gel phase was 20 times greater than that of the same amount of native enzyme in a liquid water/hexane bi-phasic system containing the same amount of water. This effect was probably due to the higher interface area between the organic and polar phases, solving the phase problem that often exists when enzymes are used to catalyze organic reactions in nonpolar organic media.

Furthermore, a discotic pyridyl amphiphile was found to coassemble with complementary carboxylic acids to form emulsion gels with porous architecture. Interestingly, this porous structure exhibited a template effect for lipase enzyme derived from *Candida rugose* (Scheme 45). The system was used to catalyze the inclusion of gastrodigenin (*p*-hydroxybenzyl alcohol) via an esterification reaction. It was demonstrated that in dependence of gel pore size, the enzymatic catalytic activity could be tuned, and different reaction products were obtained.

The enzymatic reactions were carried out into the soft material at mild aqueous-organic conditions and with a higher rate. In addition, the enzymatic reaction led the emulsion gel to separate into two phases, which resulted in recyclability of the pyridyl amphiphiles.[61]

Conclusions

The overview of data so far reported about catalysis in supramolecular gel phases sheds light on the wide potential of such kind of investigation. In most cases, the large improvements achieved in gel phases compared to solutions were obtained in terms of higher yields and shorter reaction times. These results can be directly related to the increased local concentration of the catalytic functions induced by the formation of the self-assembled gelatinous network. Never-

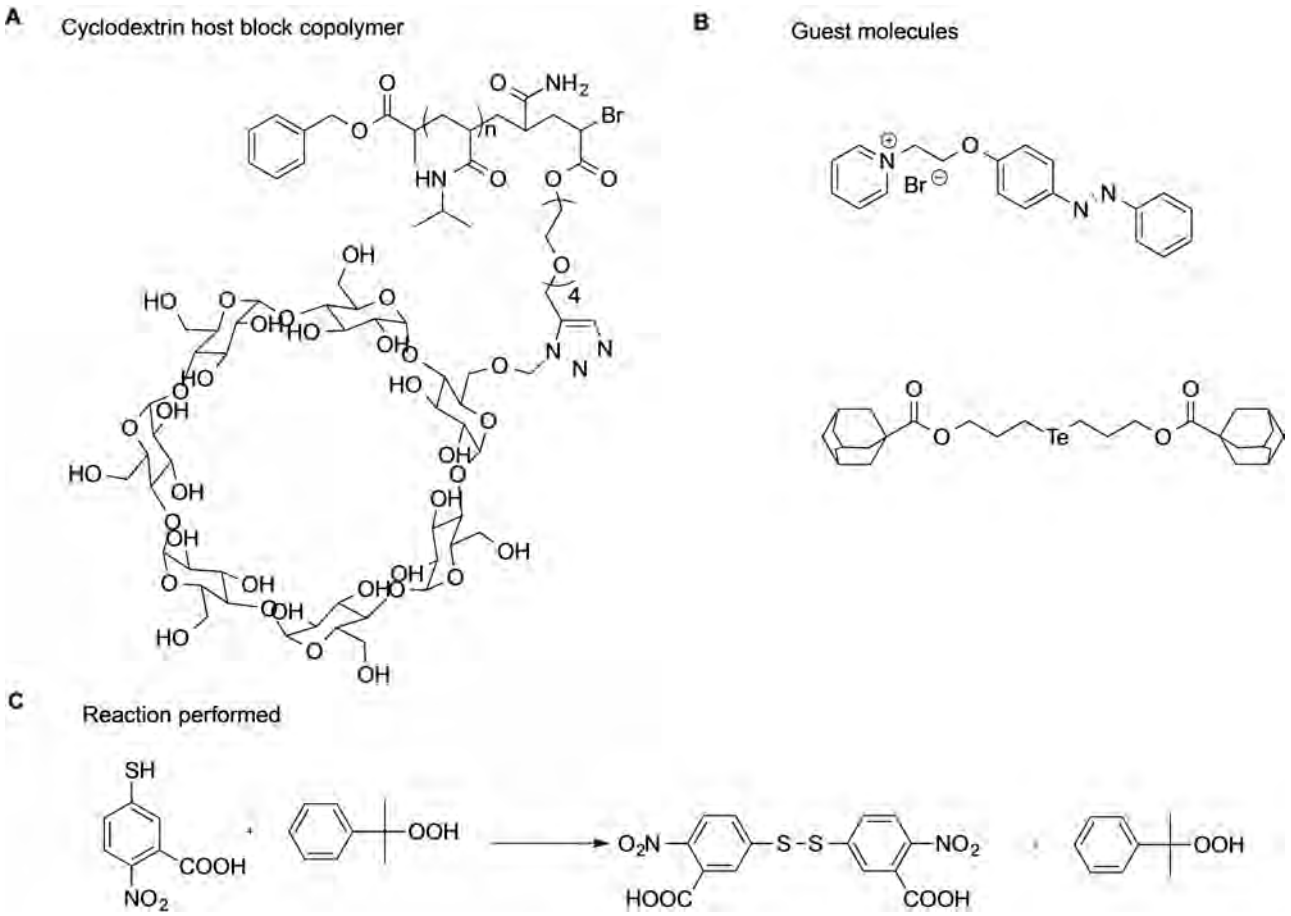

Scheme 43. A) Structure of host and **B)** guest complexes used to form gels; **C)** reduction of cumene hydroperoxide (CUOOH) with TNB (3-carboxyl-4-nitro-benzenethiol) to test the catalytic activity of the system with GPx.

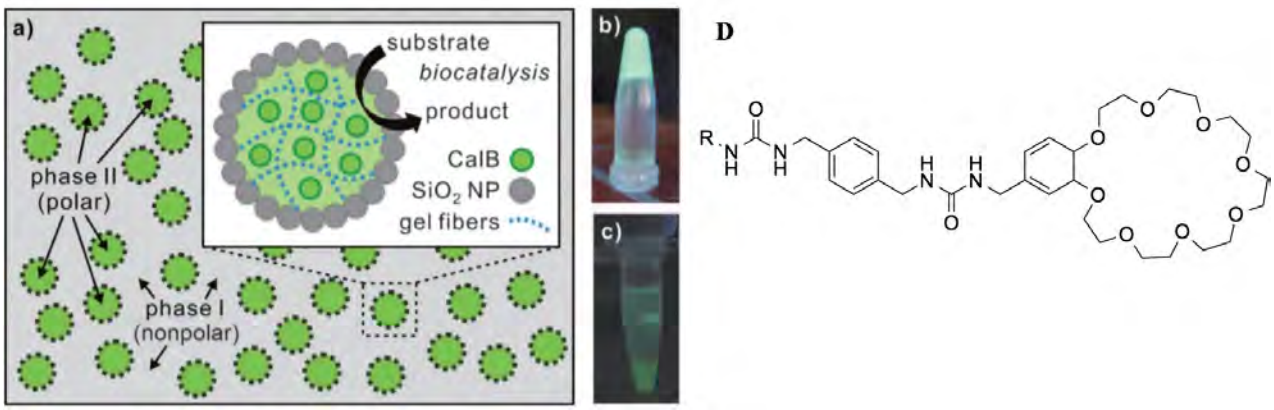

Scheme 44. A) Schematic illustration of a Pickering emulsion used for enzymatic catalysis of organic reactions. The inner polar phase II contains the enzyme (CalB) trapped in jellified microparticles that are stabilized by SiO_2 nanoparticles; **B)** gel loaded with enzyme; **C)** enzyme release upon addition of KPF_6 to the gel. Schematic representation of gel and images reproduced from Ref. [60]. **D)** Structure of gelator.

theless, this effect is frequently counterbalanced by loss in performance in the stereochemical control of the reaction, as a consequence of the increase in basicity of some catalytic functions as well as the enhanced reaction rate.

Gel phases proved to be efficient supports for metal and metal nanoparticles. The entrapment of metal species in the gelatinous network, in addition to enhance reaction yields with higher reaction rates, allows a significant reduction in metal leaching frequently featuring metal catalysis. In this sense,

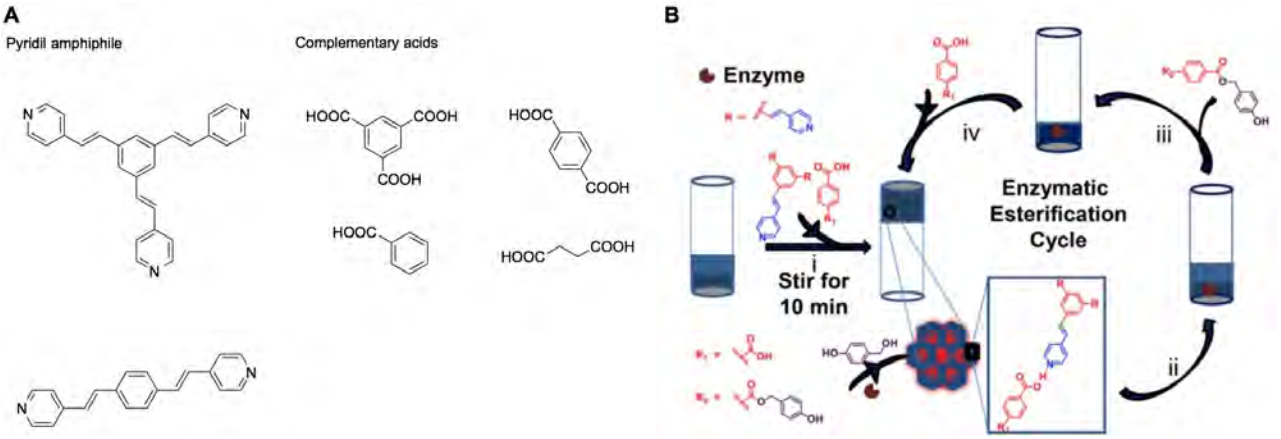

Scheme 45. A) Structure of amphiphile and carboxylic acids forming supramolecular emulsion gels; **B)** schematic representation of the enzymatic catalysis in gel. Reproduced from Ref. [61], Copyright (2018), with permission from American Chemical Society.

supramolecular gels behaved as solid supports favoring not only the achievement of good reaction yield, under mild conditions, but also the efficient recycle of the catalytic system.

Supramolecular gels have been efficiently used also as reaction media for photocatalytic processes, like the H_2 production and C–C formation. Besides the advantages in terms of conversion and yield, the main improvement deriving from the use of a gels as reaction media, stands in the possibility to carry out the reaction also under aerobic conditions without loss in performance, achieving better yields even in comparison to the reaction performed in solution under inert conditions. Indeed, the gel network proved to be efficient in shielding reactants and intermediates from deleterious effects of oxygen species. Certainly, this represents a remarkable simplification in the application of such kinds of protocols that can also be of industrial relevance.

Finally, supramolecular gels have been efficiently used as supporting phases for biocatalysis. In most cases, the enzyme entrapment in the confined gelatinous network results in a corresponding increased efficiency. This is mainly due to the fact that the gelatinous environment allows to increase the interface area between organic and polar phases, frequently representing the limiting factor of the biocatalysts used in apolar solvents.

In summary, carring out reactions in gel phases rather than in solution can give different advantages from both a kinetic and environmental point of view, like increased yields, the use of mild reaction conditions and the recyclability of the catalytic phase. Unfortunately, a full comparison cannot be performed, as reactions in solution and gel phase are seldom performed under the same experimental conditions. Furthermore, in gel phase, analysis of important parameters such as catalyst loading, TON and TOF is rarely analyzed. Then, it is desirable that such aspects will be better considered in future studies to have homogenous insights about catalytic ability of these reaction media.

As above said, this review is not an exhaustive analysis of the different catalytic applications so far reported in this area. However, it gives a clear idea of the work performed in the last decade and, considering the significant positive repercussions so far detected, can be a useful incitement for the research of new applications in the area.

Conflict of Interest

The authors declare no conflict of interest.

Keywords: Biocatalysis · Metal-catalysis · Organocatalysis · Photocatalysis · Supramolecular gels

[1] a) Q. Chen, H. Schönherr, G. J. Vancso, *Small* **2009**, *5*, 1436–1445; b) A. de la Escosura, R. J. M. Nolte, J. J. L. M. Cornelissen, *J. Mater. Chem.* **2009**, *19*, 2274–2278.
[2] B. Breiner, J. K. Clegg, J. R. Nitschke, *Chem. Sci.* **2011**, *2*, 51–56.
[3] J. K. Clegg, S. S. Iremonger, M. J. Hayter, P. D. Southon, R. B. Macquart, M. B. Duriska, P. Jensen, P. Turner, K. A. Jolliffe, C. J. Kepert, G. V. Meehan, L. F. Lindoy, *Angew. Chem. Int. Ed.* **2010**, *49*, 1075–1078; *Angew. Chem.* **2010**, *122*, 1093–1096.
[4] P. Mal, D. Schultz, K. Beyeh, K. Rissanen, J. R. Nitschke, *Angew. Chem. Int. Ed.* **2008**, *47*, 8297–8301; *Angew. Chem.* **2008**, *120*, 8421–8425.
[5] S. Wanda, P. Jerzy, *Mini-Rev. Org. Chem.* **2007**, *4*, 125–142.
[6] L. Isaacs, *Chem. Commun.* **2009**, 619–629.
[7] S. Y. Hong, R. Popovitz-Biro, G. Tobias, B. Ballesteros, B. G. Davis, M. L. H. Green, R. Tenne, *Nano Res.* **2010**, *3*, 170–173.
[8] M. Takata, B. Umeda, E. Nishibori, M. Sakata, Y. Saitot, M. Ohno, H. Shinohara, *Nature* **1995**, *377*, 46–49.
[9] L. Schiaffino, G. Ercolani, *Angew. Chem. Int. Ed.* **2008**, *47*, 6832–6835; *Angew. Chem.* **2008**, *120*, 6938–6941.
[10] a) J. Bachl, S. Oehm, J. Mayr, C. Cativiela, J. J. Marrero-Tellado, D. Díaz Díaz, *Int. J. Mol. Sci.* **2015**, *16*, 11766–11784; b) C. Rizzo, J. L. Andrews, J. W. Steed, F. D'Anna, *J. Colloid Interface Sci.* **2019**, *548*, 184–196; c) C. Rizzo, A. Mandoli, S. Marullo, F. D'Anna, *J. Org. Chem.* **2019**, *84*, 6356–6365; d) C. Rizzo, S. Marullo, P. R. Campodonico, I. Pibiri, N. T. Dintcheva, R. Noto, D. Millan, F. D'Anna, *ACS Sustainable Chem. Eng.* **2018**, *6*, 12453–12462; e) C. Rizzo, S. Marullo, F. D'Anna, *Environ. Sci.-Nano* **2021**, *8*, 131–145; f) Y. Wang, Y. Wang, X. Yan, S. Wu, L. Shao, Y. Liu, Z. Guo, *Chemosphere* **2016**, *153*, 485–493; g) Y. Wang, S. Wu, X. Yan, T. Ma, L. Shao, Y. Liu, Z. Guo, *Chemosphere* **2017**, *167*, 178–187; h) L. Yan, G. Li, Z. Ye, F. Tian, S. Zhang, *Chem. Commun.* **2014**, *50*, 14839–14842; i) B. Zhang, S. Chen, H. Luo, B. Zhang, F. Wang, J. Song, *J. Hazard. Mater.* **2020**, *384*, 121460.

[11] F. Billeci, F. D'Anna, H. Q. N. Gunaratne, N. V. Plechkova, K. R. Seddon, *Green Chem.* **2018**, *20*, 4260–4276.
[12] a) X. Cao, A. Gao, J.-t. Hou, T. Yi, *Coord. Chem. Rev.* **2021**, *434*, 213792; b) S. Panja, A. Panja, K. Ghosh, *Mater. Chem. Front.* **2021**, *5*, 584–602; c) C. Wang, Q. Han, P. Liu, G. Zhang, L. Song, X. Zou, Y. Fu, *ACS Sens.* **2021**, *6*, 252–258.
[13] a) N. Falcone, T. Shao, N. M. O. Andoy, R. Rashid, R. M. A. Sullan, X. Sun, H.-B. Kraatz, *Biomater. Sci.* **2020**, *8*, 5601–5614; b) J. Hu, Q. Hu, X. He, C. Liu, Y. Kong, Y. Cheng, Y. Zhang, *Adv. Healthcare Mater.* **2020**, *9*, 1901329; c) S. S. E. Michel, A. Kilner, J.-C. Eloi, S. E. Rogers, W. H. Briscoe, M. C. Galan, *ACS Appl. Bio Mater.* **2020**, *3*, 5253–5262; d) A. K. Patterson, D. K. Smith, *Chem. Commun.* **2020**, *56*, 11046–11049; e) C. C. Piras, C. S. Mahon, D. K. Smith, *Chem. Eur. J.* **2020**, *26*, 8452–8457.
[14] a) A. Dawn, *Int. J. Mol. Sci.* **2019**, *20*, 781; b) J. A. Foster, J. W. Steed, *Angew. Chem. Int. Ed.* **2010**, *49*, 6718–6724; *Angew. Chem.* **2010**, *122*, 6868–6874; c) Q. Jin, L. Zhang, H. Cao, T. Wang, X. Zhu, J. Jiang, M. Liu, *Langmuir* **2011**, *27*, 13847–13853; d) B. Maiti, A. Abramov, R. Pérez-Ruiz, D. Díaz Díaz, *Acc. Chem. Res.* **2019**, *52*, 1865–1876; e) R. Pérez-Ruiz, D. Díaz Díaz, *Soft Matter* **2015**, *11*, 5180–5187.
[15] F. Rodríguez-Llansola, J. F. Miravet, B. Escuder, *Chem. Commun.* **2009**, 7303–7305.
[16] F. Rodríguez-Llansola, B. Escuder, J. F. Miravet, *Org. Biomol. Chem.* **2009**, *7*, 3091–3094.
[17] M. Tena-Solsona, J. Nanda, S. Díaz-Oltra, A. Chotera, G. Ashkenasy, B. Escuder, *Chem. Eur. J.* **2016**, *22*, 6687–6694.
[18] N. Singh, K. Zhang, C. A. Angulo-Pachón, E. Mendes, J. H. van Esch, B. Escuder, *Chem. Sci.* **2016**, *7*, 5568–5572.
[19] K. Hawkins, A. K. Patterson, P. A. Clarke, D. K. Smith, *J. Am. Chem. Soc.* **2020**, *142*, 4379–4389.
[20] F. Rodríguez-Llansola, B. Escuder, J. F. Miravet, *J. Am. Chem. Soc.* **2009**, *131*, 11478–11484.
[21] F. Rodríguez-Llansola, J. F. Miravet, B. Escuder, *Chem. Eur. J.* **2010**, *16*, 8480–8486.
[22] N. Singh, B. Escuder, *Chem. Eur. J.* **2017**, *23*, 9946–9951.
[23] E.-M. Schön, E. Marqués-López, R. P. Herrera, C. Alemán, D. D. Díaz, *Chem. Eur. J.* **2014**, *20*, 10720–10731.
[24] R. Porcar, M. I. Burguete, P. Lozano, E. Garcia-Verdugo, S. V. Luis, *ACS Sustainable Chem. Eng.* **2016**, *4*, 6062–6071.
[25] E.-M. Schön, C. Saldías, D. Haldar, D. Díaz, *Macromol. Symp.* **2019**, *385*, 1800193.
[26] N. Singh, M. P. Conte, R. V. Ulijn, J. F. Miravet, B. Escuder, *Chem. Commun.* **2015**, *51*, 13213–13216.
[27] S. Kawamorita, M. Fujiki, Z. Li, T. Kitagawa, Y. Imada, T. Naota, *ChemCatChem* **2019**, *11*, 878–884.
[28] M. Araújo, S. Díaz-Oltra, B. Escuder, *Chem. Eur. J.* **2016**, *22*, 8676–8684.
[29] M. Araújo, I. Muñoz Capdevila, S. Díaz-Oltra, B. Escuder, *Molecules* **2016**, *21*.
[30] M. Araújo, B. Escuder, *ChemistrySelect* **2017**, *2*, 854–862.
[31] G. Wang, D. Wang, J. Bietsch, A. Chen, P. Sharma, *J. Org. Chem.* **2020**, *85*, 16136–16156.
[32] J. R. Hiscock, G. P. Bustone, E. R. Clark, *ChemistryOpen* **2017**, *6*, 497–500.
[33] B. Adhikari, A. Biswas, A. Banerjee, *ACS Appl. Mater. Interfaces* **2012**, *4*, 5472–5482.
[34] M. Paul, K. Sarkar, P. Dastidar, *Chem. Eur. J.* **2015**, *21*, 255–268.
[35] P. Slavík, D. W. Kurka, D. K. Smith, *Chem. Sci.* **2018**, *9*, 8673–8681.
[36] C. C. Piras, P. Slavik, D. K. Smith, *Angew. Chem. Int. Ed.* **2020**, *59*, 853–859; *Angew. Chem.* **2020**, *132*, 863–869.
[37] P. Slavik, D. K. Smith, *Tetrahedron* **2020**, *76*, 131344.
[38] P.-F. Vittoz, H. El Siblani, A. Bruma, B. Rigaud, X. Sauvage, C. Fernandez, A. Vicente, N. Barrier, S. Malo, J. Levillain, A.-C. Gaumont, I. Dez, *ACS Sustainable Chem. Eng.* **2018**, *6*, 5192–5197.
[39] K. M. Bothwell, F. Lorenzini, E. Mathers, P. C. Marr, A. C. Marr, *ACS Sustainable Chem. Eng.* **2019**, *7*, 2686–2690.
[40] S. Kumari, M. Häring, S. S. Gupta, D. Díaz Díaz, *ChemPlusChem* **2017**, *82*, 225–232.
[41] S. D. Kurbah, R. A. Lal, *New J. Chem.* **2020**, *44*, 5410–5418.
[42] a) M. Freitag, N. Möller, A. Rühling, C. A. Strassert, B. J. Ravoo, F. Glorius, *ChemPhotoChem* **2019**, *3*, 24–27; b) B. D. Ravetz, A. B. Pun, E. M. Churchill, D. N. Congreve, T. Rovis, L. M. Campos, *Nature* **2019**, *565*, 343–346.
[43] T. N. Singh-Rachford, F. N. Castellano, *Coord. Chem. Rev.* **2010**, *254*, 2560–2573.
[44] P. Duan, N. Yanai, H. Nagatomi, N. Kimizuka, *J. Am. Chem. Soc.* **2015**, *137*, 1887–1894.
[45] M. Häring, R. Pérez-Ruiz, A. Jacobi von Wangelin, D. D. Díaz, *Chem. Commun.* **2015**, *51*, 16848–16851.
[46] M. Häring, A. Abramov, K. Okumura, I. Ghosh, B. König, N. Yanai, N. Kimizuka, D. Díaz Díaz, *J. Org. Chem.* **2018**, *83*, 7928–7938.
[47] J. C. Herrera-Luna, D. Díaz Díaz, A. Abramov, S. Encinas, M. C. Jiménez, R. Pérez-Ruiz, *Org. Lett.* **2021**, *23*, 2320–2325.
[48] A. Abramov, H. Vernickel, C. Saldías, D. Díaz Díaz, *Molecules* **2019**, *24*.
[49] G. Yang, C. Lin, X. Feng, T. Wang, J. Jiang, *Chem. Commun.* **2020**, *56*, 527–530.
[50] P. Liao, Y. Hu, Z. Liang, J. Zhang, H. Yang, L.-Q. He, Y.-X. Tong, J.-M. Liu, L. Chen, C.-Y. Su, *J. Mater. Chem. A* **2018**, *6*, 3195–3201.
[51] A. S. Weingarten, R. V. Kazantsev, L. C. Palmer, D. J. Fairfield, A. R. Koltonow, S. I. Stupp, *J. Am. Chem. Soc.* **2015**, *137*, 15241–15246.
[52] S. Das, N. Okamura, S. Yagi, A. Ajayaghosh, *J. Am. Chem. Soc.* **2019**, *141*, 5635–5639.
[53] S. Bhat, U. Maitra, *Molecules* **2007**, *12*, 2181–2189.
[54] a) A. Dawn, N. Fujita, S. Haraguchi, K. Sada, S.-i. Tamaru, S. Shinkai, *Org. Biomol. Chem.* **2009**, *7*, 4378–4385; b) A. Dawn, N. Fujita, S. Haraguchi, K. Sada, S. Shinkai, *Chem. Commun.* **2009**, 2100–2102.
[55] J. Bachl, A. Hohenleutner, B. B. Dhar, C. Cativiela, U. Maitra, B. König, D. D. Díaz, *J. Mater. Chem. A* **2013**, *1*, 4577–4588.
[56] A. R. Hirst, S. Roy, M. Arora, A. K. Das, N. Hodson, P. Murray, S. Marshall, N. Javid, J. Sefcik, J. Boekhoven, J. H. van Esch, S. Santabarbara, N. T. Hunt, R. V. Ulijn, *Nat. Chem.* **2010**, *2*, 1089–1094.
[57] J. W. Sadownik, J. Leckie, R. V. Ulijn, *Chem. Commun.* **2011**, *47*, 728–730.
[58] Y. Yin, S. Jiao, C. Lang, J. Liu, *Soft Matter* **2014**, *10*, 3374–3385.
[59] Y. Yin, S. Jiao, R. Zhang, X. Hu, Z. Shi, Z. Huang, *Soft Matter* **2015**, *11*, 5301–5312.
[60] Z. Qi, C. Wu, P. Malo de Molina, H. Sun, A. Schulz, C. Griesinger, M. Gradzielski, R. Haag, M. B. Ansorge-Schumacher, C. A. Schalley, *Chem. Eur. J.* **2013**, *19*, 10150–10159.
[61] S. Biswas, R. G. Jadhav, A. K. Das, *ACS Appl. Nano Mater.* **2018**, *1*, 175–182.

Manuscript received: March 25, 2021
Revised manuscript received: May 7, 2021
Accepted manuscript online: May 12, 2021